University of Nottingham
UK | CHINA | MALAYSIA

G2TRC GAS TURBINE AND TRANSMISSIONS RESEARCH CENTRE

Bubble Dissolution in Taylor-Couette flow

Gabriele Gennari
Dr. Richard Jefferson-Loveday

BGUM 2023
July 6th, Paris

Department of Mechanical, Materials and Manufacturing Engineering, University of Nottingham, Nottingham NG7 2RD, United Kingdom

Outline

1. Motivation
2. Description of the problem
3. Numerical Framework
4. Taylor-Couette flow: single-phase validation
5. Mass transfer in Taylor-Couette flow
6. Conclusions

Motivation

Mass transfer of soluble species

- Mass transfer of soluble species occurs in many natural and industrial systems.

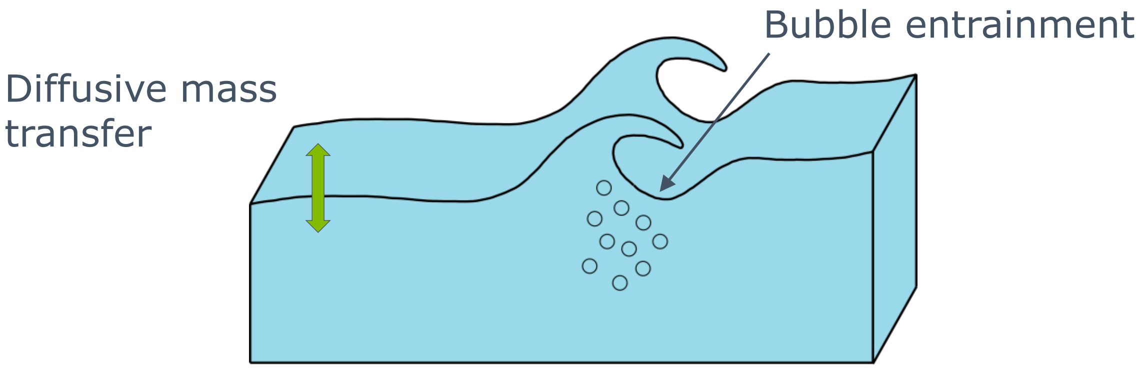

- Air-Sea gas transfer

- Chemical reactors
- Green production of hydrogen

- Complex physics (multi-phase flow, interfacial discontinuity, reactive species).
- Design models rely on simplified correlation formulae.

Problem description

Soluble species in bubbly flows

- Disperse bubbly flow
- Soluble species in the liquid

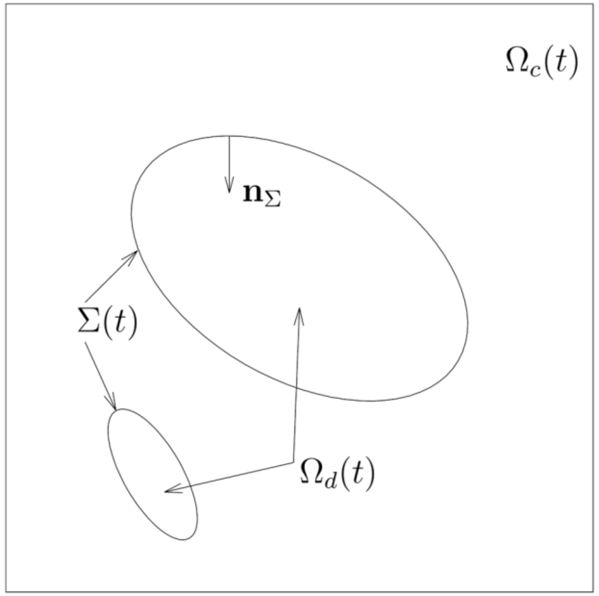

Problem description

Soluble species in bubbly flows

- Disperse bubbly flow
- Soluble species in the liquid

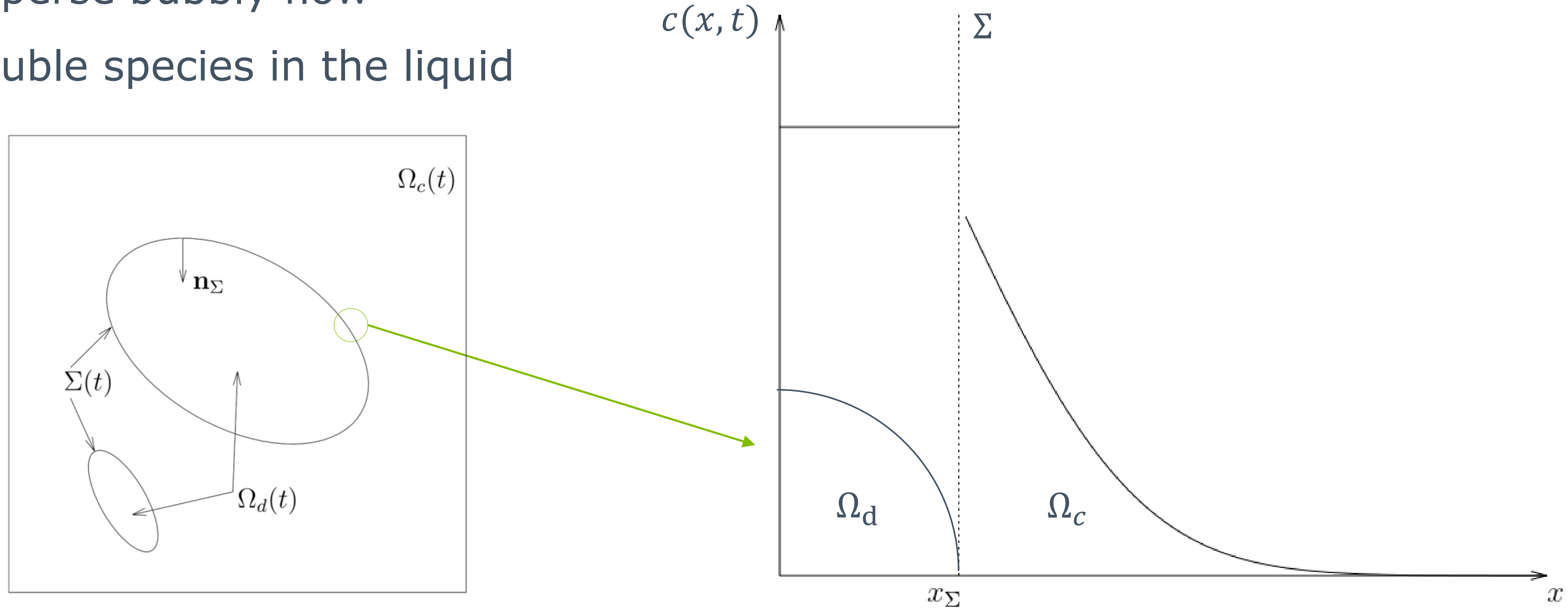

Problem description

Soluble species in bubbly flows

- Disperse bubbly flow
- Soluble species in the liquid

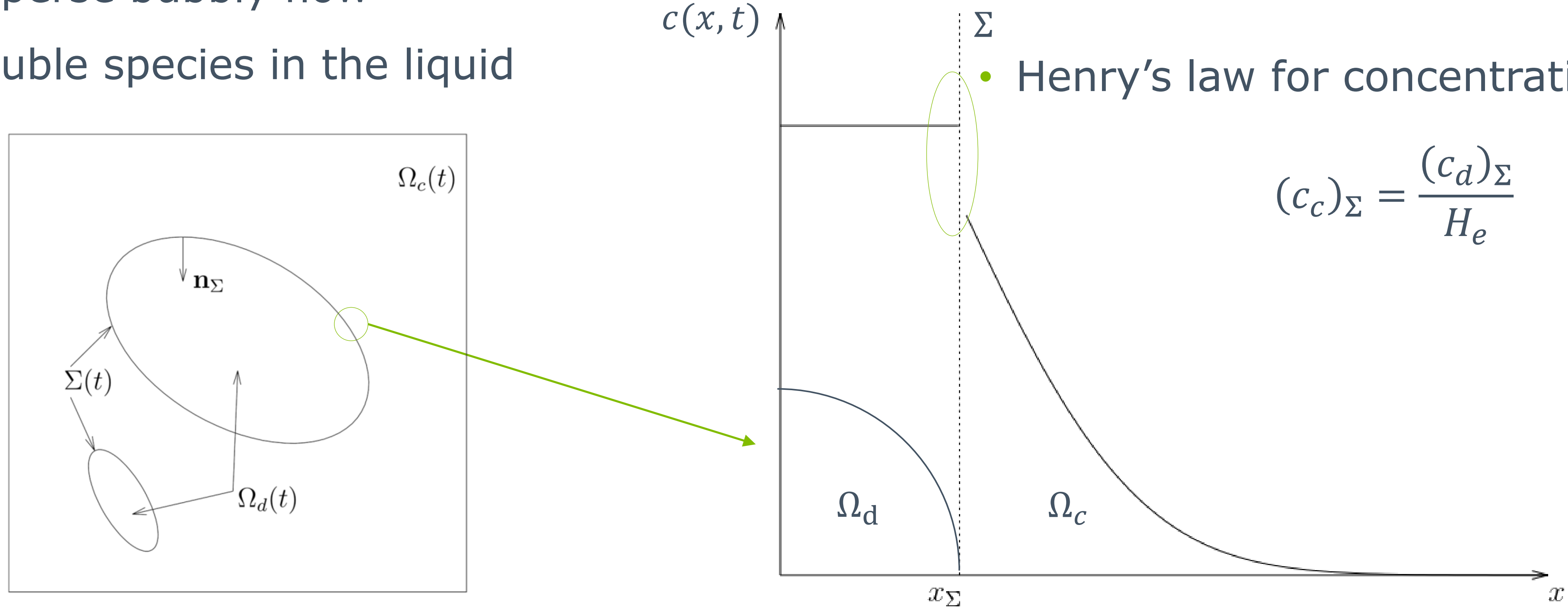

- Henry's law for concentration jump

$$(c_c)_\Sigma = \frac{(c_d)_\Sigma}{H_e}$$

Numerical framework

Direct Numerical Simulations of two-phase flows

- Incompressible DNS + geometric VOF
- Phase-change model

$$\nabla \cdot \boldsymbol{u} = \dot{m}\left(\frac{1}{\rho_d} - \frac{1}{\rho_c}\right)\delta_\Sigma$$

$$\frac{\partial \boldsymbol{u}}{\partial t} + \nabla \cdot (\boldsymbol{u} \otimes \boldsymbol{u}) = \frac{1}{\rho}\left[-\nabla p + \nabla \cdot (2\mu \boldsymbol{D})\right] + \frac{\sigma k \boldsymbol{n}_\Sigma}{\rho}\delta_\Sigma$$

$$\frac{\partial f}{\partial t} + \nabla \cdot (\boldsymbol{u} f) = -\frac{\dot{m}}{\rho_c}\delta_\Sigma$$

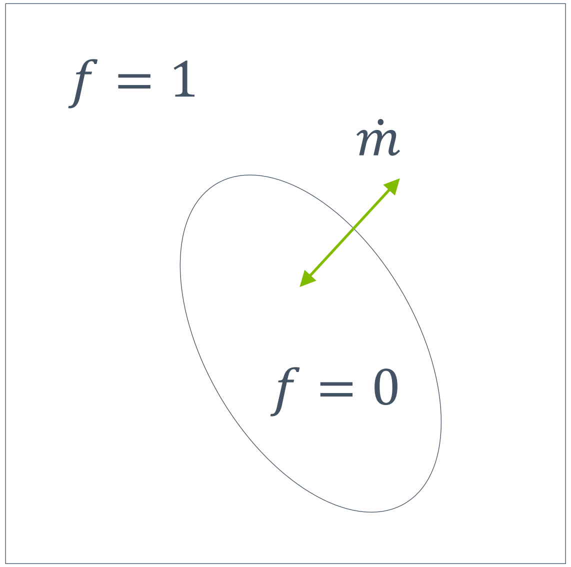

Transport of species

Two-scalar approach

- Two scalar equations for each species

$$\frac{\phi_c^{n+1}-\phi_c^n}{\Delta t}V+\oint_{\partial V_c\setminus\Sigma} c_c\boldsymbol{u}_c\cdot\boldsymbol{n}\,ds-\oint_{\partial V_c\setminus\Sigma} D_c\nabla c_c\cdot\boldsymbol{n}\,ds=-\oint_{\Sigma}\frac{\dot{m}}{M}\,ds$$

$$\frac{\phi_d^{n+1}-\phi_d^n}{\Delta t}V+\oint_{\partial V_d\setminus\Sigma} c_d\boldsymbol{u}_{\boldsymbol{d}}\cdot\boldsymbol{n}\,ds-\oint_{\partial V_d\setminus\Sigma} D_d\nabla c_d\cdot\boldsymbol{n}\,ds=+\oint_{\Sigma}\frac{\dot{m}}{M}\,ds$$

Transport of species

Two-scalar approach

- Two scalar equations for each species

- Species confined within the respective phase during advection/diffusion
- Advection: tracers associated to VOF field
- Diffusion coefficient weighted by the face fraction field [*]

$$\frac{\phi_c^{n+1} - \phi_c^n}{\Delta t} V + \oint_{\partial V_c \setminus \Sigma} c_c \boldsymbol{u}_c \cdot \boldsymbol{n}\, ds - \oint_{\partial V_c \setminus \Sigma} D_c \nabla c_c \cdot \boldsymbol{n}\, ds = -\oint_{\Sigma} \frac{\dot{m}}{M}\, ds$$

$$\frac{\phi_d^{n+1} - \phi_d^n}{\Delta t} V + \oint_{\partial V_d \setminus \Sigma} c_d \boldsymbol{u}_d \cdot \boldsymbol{n}\, ds - \oint_{\partial V_d \setminus \Sigma} D_d \nabla c_d \cdot \boldsymbol{n}\, ds = +\oint_{\Sigma} \frac{\dot{m}}{M}\, ds$$

Mass conservation

* Magdelaine-Guillot de Suduiraut, Q., 2019. Hydrodynamique des films liquides hétérogènes. Thesis. Sorbonne Université.

Mass transfer rate

A geometric scheme

- Diffusion-driven mass transfer (Fick's law)
- $\dot{m} = -\frac{D_c M}{1-y}\frac{\partial c_c}{\partial \boldsymbol{n}_\Sigma}$

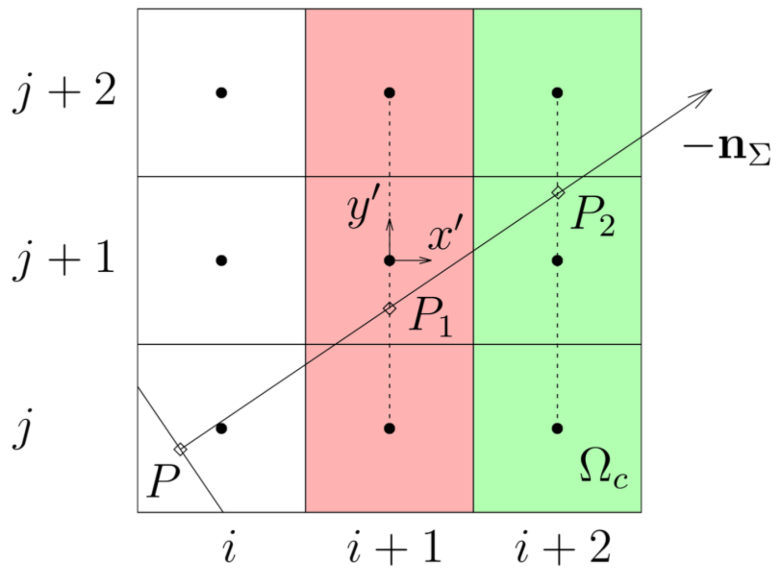

- $-\frac{\partial c_c}{\partial \boldsymbol{n}_\Sigma} = f_P \frac{c_c(P_1)-c_c(P)}{PP_1} + (1-f_P)\frac{c_c(P_2)-c_c(P)}{PP_2}$ [*]
- $c_c(P) = \frac{c_d(P)}{H_e}$ (Henry's law)

* Bothe, D., Fleckenstein, S., 2013. A volume-of-fluid-based method for mass transfer processes at fluid particles. Chem. Eng. Sci. 101, 283–302.

Mass transfer rate

A geometric scheme

- Diffusion-driven mass transfer (Fick's law)
- $\dot{m} = -\frac{D_c M}{1-y}\frac{\partial c_c}{\partial \boldsymbol{n}_\Sigma}$

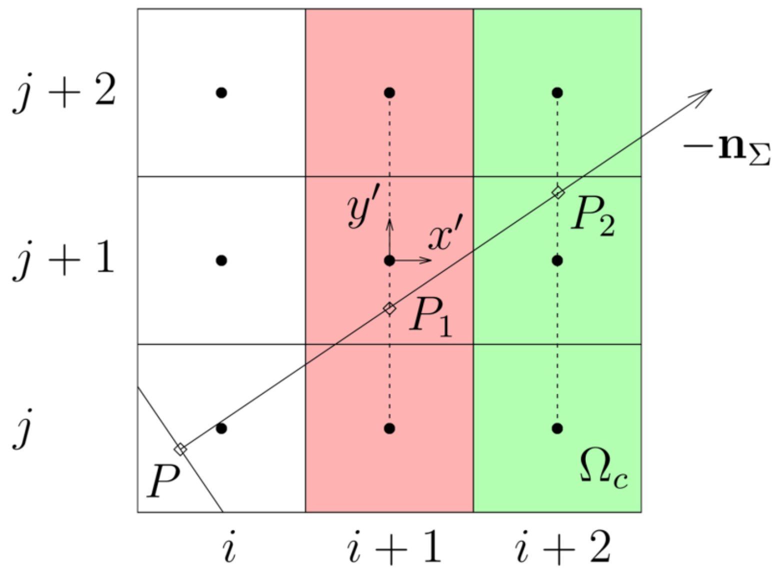

- $-\frac{\partial c_c}{\partial \boldsymbol{n}_\Sigma} = f_P \frac{c_c(P_1)-c_c(P)}{PP_1} + (1-f_P)\frac{c_c(P_2)-c_c(P)}{PP_2}$ [*]
- $c_c(P) = \frac{c_d(P)}{H_e}$ (Henry's law)

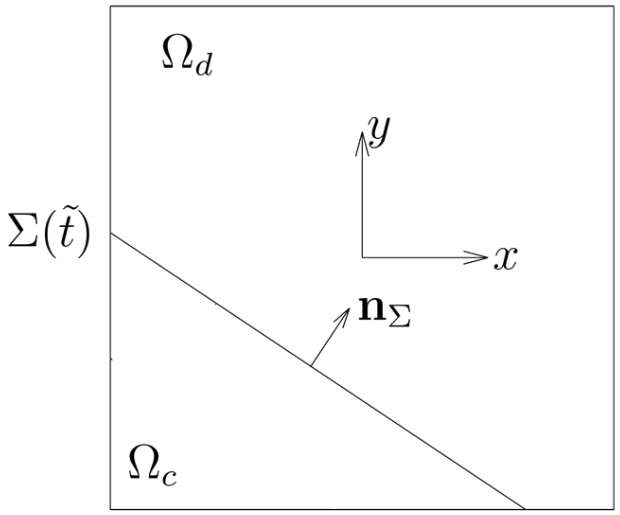

$$\frac{\partial f}{\partial t} + \nabla \cdot (\boldsymbol{u} f) = -\frac{\dot{m}}{\rho_c}\delta_\Sigma$$

* Bothe, D., Fleckenstein, S., 2013. A volume-of-fluid-based method for mass transfer processes at fluid particles. Chem. Eng. Sci. 101, 283–302.

Mass transfer rate

A geometric scheme

- Diffusion-driven mass transfer (Fick's law)
- $\dot{m} = -\frac{D_c M}{1-y}\frac{\partial c_c}{\partial \boldsymbol{n}_\Sigma}$

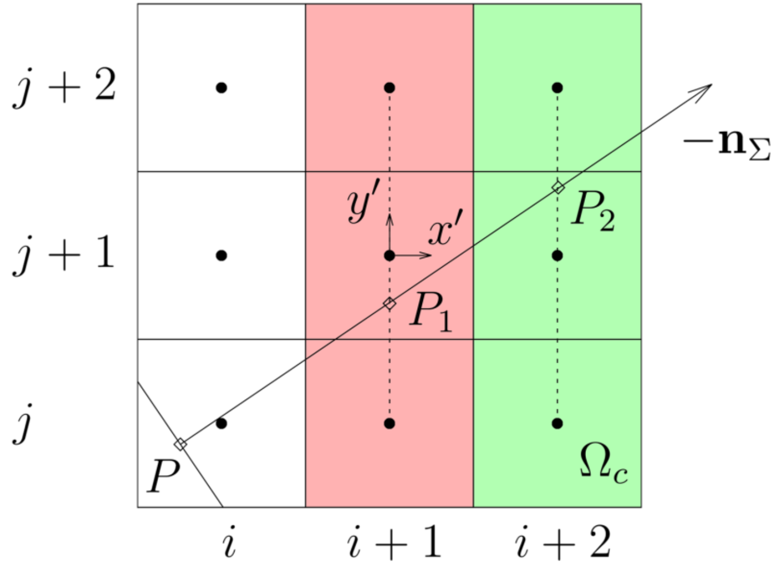

- $-\frac{\partial c_c}{\partial \boldsymbol{n}_\Sigma} = f_P \frac{c_c(P_1)-c_c(P)}{PP_1} + (1-f_P)\frac{c_c(P_2)-c_c(P)}{PP_2}$ [*]
- $c_c(P) = \frac{c_d(P)}{H_e}$ (Henry's law)

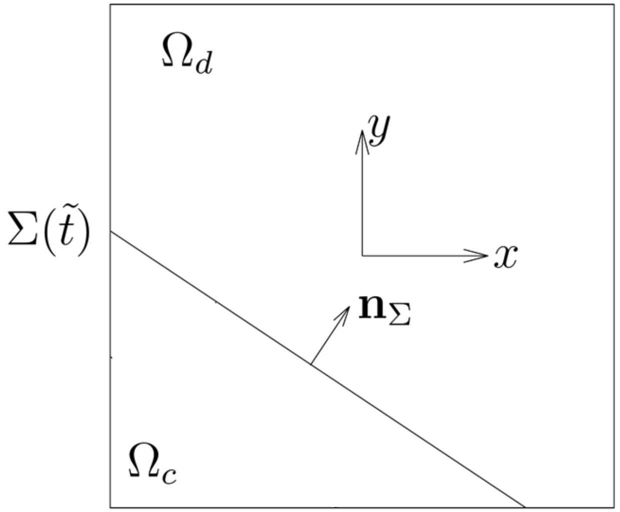

$$\frac{\partial f}{\partial t} + \nabla\cdot(\boldsymbol{u}f) = -\frac{\dot{m}}{\rho_c}\delta_\Sigma$$

$$\boldsymbol{h}_\Sigma = -\frac{\dot{m}}{\rho_c}\frac{\Delta t}{\Delta}\boldsymbol{n}_\Sigma$$

* Bothe, D., Fleckenstein, S., 2013. A volume-of-fluid-based method for mass transfer processes at fluid particles. Chem. Eng. Sci. 101, 283–302.

Mass transfer rate

A geometric scheme

- Diffusion-driven mass transfer (Fick's law)
- $\dot{m} = -\frac{D_c M}{1-y} \frac{\partial c_c}{\partial \boldsymbol{n}_\Sigma}$
- $-\frac{\partial c_c}{\partial \boldsymbol{n}_\Sigma} = f_P \frac{c_c(P_1) - c_c(P)}{PP_1} + (1 - f_P) \frac{c_c(P_2) - c_c(P)}{PP_2}$ [*]
- $c_c(P) = \frac{c_d(P)}{H_e}$ (Henry's law)

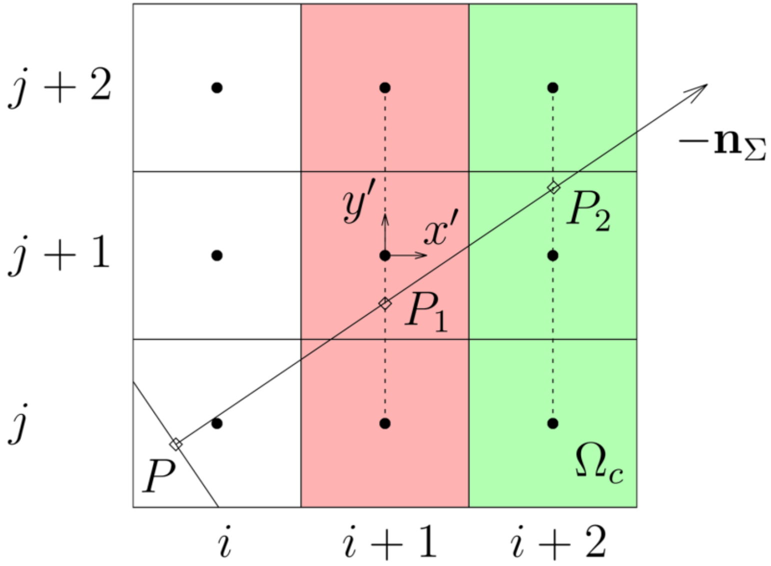

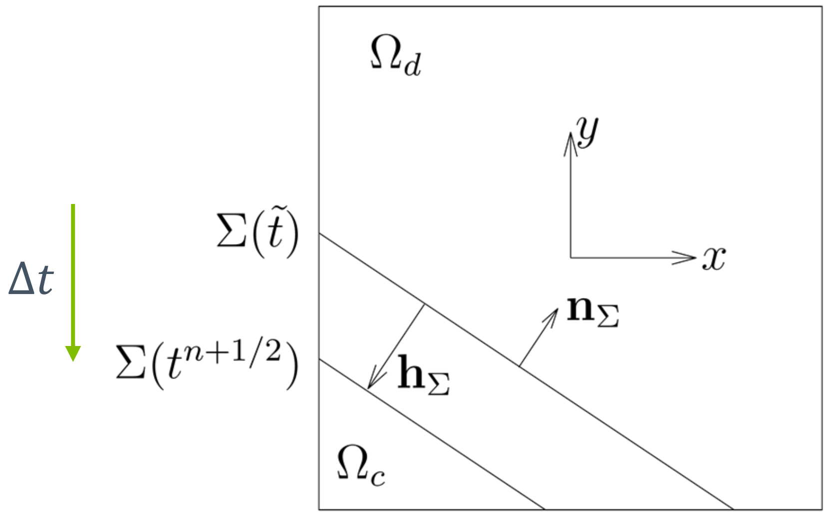

$$\frac{\partial f}{\partial t} + \nabla \cdot (\boldsymbol{u} f) = -\frac{\dot{m}}{\rho_c} \delta_\Sigma$$

$$\boldsymbol{h}_\Sigma = -\frac{\dot{m}}{\rho_c} \frac{\Delta t}{\Delta} \boldsymbol{n}_\Sigma$$

* Bothe, D., Fleckenstein, S., 2013. A volume-of-fluid-based method for mass transfer processes at fluid particles. Chem. Eng. Sci. 101, 283–302.

Coupling with a geometric VOF method

Incompatibility issue

- Geometric VOF method [*]
- Kinematic constraint:

$$\frac{\Delta t}{\Delta} H_{(i,j)} \nabla_{\Delta} \cdot \boldsymbol{u} = 0$$

$$H_{(i,j)} = \begin{cases} 1 & \text{if } f > 0.5 \\ 0 & \text{Otherwise} \end{cases}$$

* Weymouth, G.D., Yue, D.K.P., 2010. Conservative volume-of-fluid method for free-surface simulations on cartesian-grids. J. Comput. Phys. 229, 2853–2865.

Coupling with a geometric VOF method

Incompatibility issue

- Geometric VOF method [*]
- Kinematic constraint:

$$\frac{\Delta t}{\Delta} H_{(i,j)} \nabla_\Delta \cdot \boldsymbol{u} = 0$$

$$H_{(i,j)} = \begin{cases} 1 & \text{if } f > 0.5 \\ 0 & \text{Otherwise} \end{cases}$$

- Always true for incompressible flows without mass transfer

* Weymouth, G.D., Yue, D.K.P., 2010. Conservative volume-of-fluid method for free-surface simulations on cartesian-grids. J. Comput. Phys. 229, 2853–2865.

Coupling with a geometric VOF method

Incompatibility issue

- Geometric VOF method [*]
- Kinematic constraint:

$$\frac{\Delta t}{\Delta} H_{(i,j)} \nabla_\Delta \cdot \boldsymbol{u} = 0$$

$$H_{(i,j)} = \begin{cases} 1 & \text{if } f > 0.5 \\ 0 & \text{Otherwise} \end{cases}$$

- Always true for incompressible flows without mass transfer
- Not true for phase-change flows

* Weymouth, G.D., Yue, D.K.P., 2010. Conservative volume-of-fluid method for free-surface simulations on cartesian-grids. J. Comput. Phys. 229, 2853–2865.

Coupling with a geometric VOF method

Incompatibility issue

Bubble with constant mass transfer rate

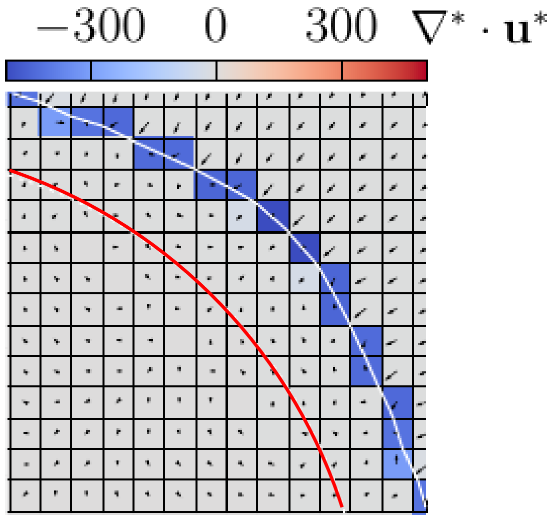

- Geometric VOF method [*]
- Kinematic constraint:

$$\frac{\Delta t}{\Delta} H_{(i,j)} \nabla_{\Delta} \cdot \boldsymbol{u} = 0$$

$$H_{(i,j)} = \begin{cases} 1 & \text{if } f > 0.5 \\ 0 & \text{Otherwise} \end{cases}$$

- Always true for incompressible flows without mass transfer
- Not true for phase-change flows

* Weymouth, G.D., Yue, D.K.P., 2010. Conservative volume-of-fluid method for free-surface simulations on cartesian-grids. J. Comput. Phys. 229, 2853–2865.

Coupling with a geometric VOF method

Incompatibility issue

- Geometric VOF method [*]
- Kinematic constraint:

$$\frac{\Delta t}{\Delta} H_{(i,j)} \nabla_{\Delta} \cdot \boldsymbol{u} = 0$$

$$H_{(i,j)} = \begin{cases} 1 & \text{if } f > 0.5 \\ 0 & \text{Otherwise} \end{cases}$$

- Always true for incompressible flows without mass transfer
- Not true for phase-change flows

Bubble with constant mass transfer rate

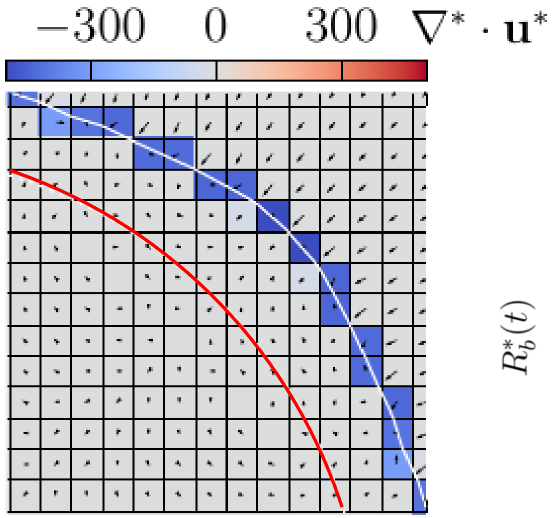

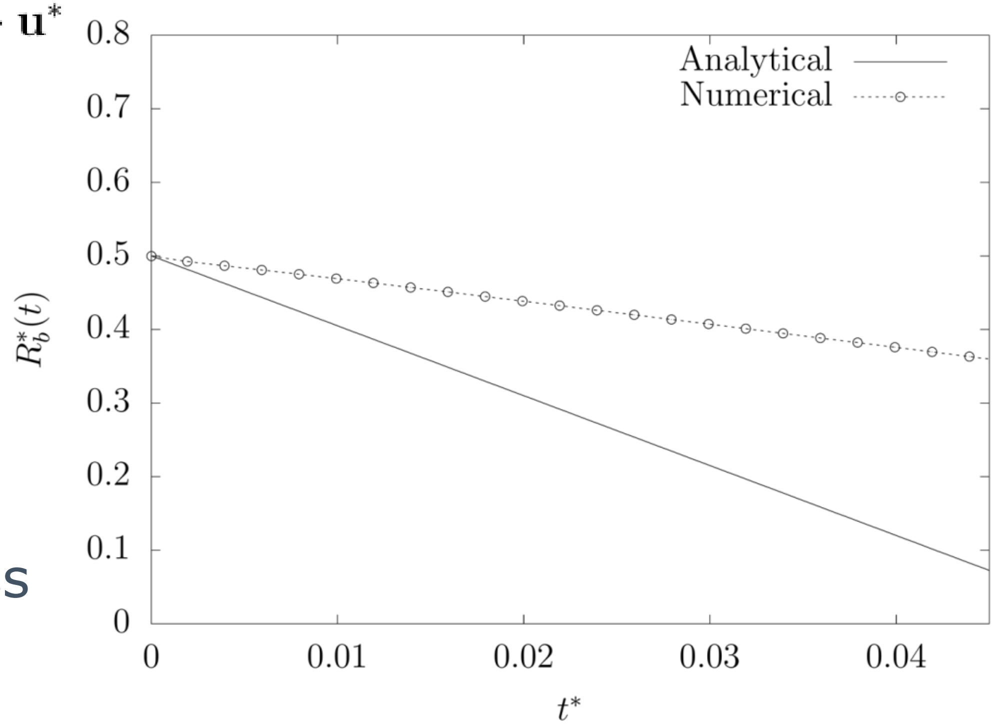

* Weymouth, G.D., Yue, D.K.P., 2010. Conservative volume-of-fluid method for free-surface simulations on cartesian-grids. J. Comput. Phys. 229, 2853–2865.

Coupling with a geometric VOF method

Velocity extension

- Always true in pure gas cells ($H_{(i,j)} = 0$)

$$\frac{\Delta t}{\Delta} H_{(i,j)} \nabla_{\Delta} \cdot \boldsymbol{u} = 0$$

Coupling with a geometric VOF method

Velocity extension

- Always true in pure gas cells ($H_{(i,j)} = 0$)

$$\frac{\Delta t}{\Delta} H_{(i,j)} \nabla_{\Delta} \cdot \boldsymbol{u} = 0$$

- Mass transfer redistribution [*,**]

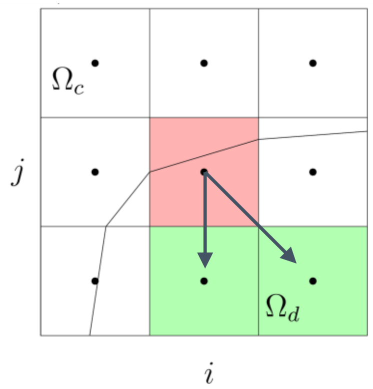

* Gennari, G., Jefferson-Loveday, R., Pickering, S. J., 2022. A phase-change model for diffusion-driven mass transfer problems in incompressible two-phase flows. Chem. Eng. Sci. 259 117791.
** Boyd, B., Ling, Y., 2023. A consistent volume-of-fluid approach for direct numerical simulation of the aerodynamic breakup of a vaporizing drop. Computers & Fluids 254 105807.

Coupling with a geometric VOF method

Velocity extension

- Always true in pure gas cells ($H_{(i,j)} = 0$)

$$\frac{\Delta t}{\Delta} H_{(i,j)} \nabla_{\Delta} \cdot \boldsymbol{u} = 0$$

- Mass transfer redistribution [*,**]

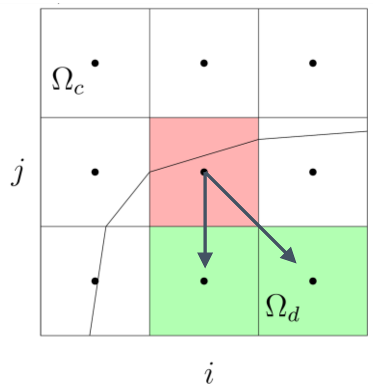

$$avg_{(i,j)} = \text{pure gas cells}\Big|_{3\times 3}$$

* Gennari, G., Jefferson-Loveday, R., Pickering, S. J., 2022. A phase-change model for diffusion-driven mass transfer problems in incompressible two-phase flows. Chem. Eng. Sci. 259 117791.
** Boyd, B., Ling, Y., 2023. A consistent volume-of-fluid approach for direct numerical simulation of the aerodynamic breakup of a vaporizing drop. Computers & Fluids 254 105807.

Coupling with a geometric VOF method

Velocity extension

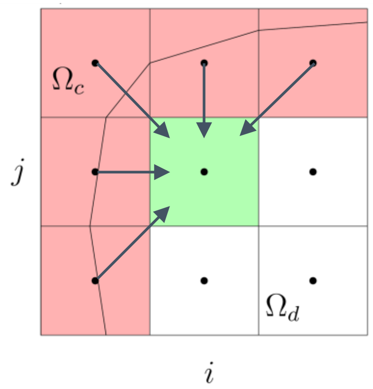

$$\dot{m}'_{(i,j)} = \sum_{3\times3} \frac{\dot{m}_{(l,k)}}{avg_{(l,k)}} A_{\Sigma(l,k)}$$

- Always true in pure gas cells ($H_{(i,j)} = 0$)

$$\frac{\Delta t}{\Delta} H_{(i,j)} \nabla_\Delta \cdot \boldsymbol{u} = 0$$

- Mass transfer redistribution [*,**]

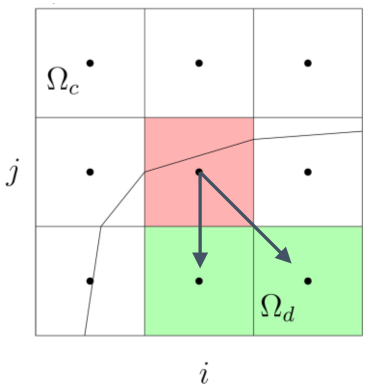

$$avg_{(i,j)} = \text{pure gas cells}\Big|_{3\times3}$$

* Gennari, G., Jefferson-Loveday, R., Pickering, S. J., 2022. A phase-change model for diffusion-driven mass transfer problems in incompressible two-phase flows. Chem. Eng. Sci. 259 117791.
** Boyd, B., Ling, Y., 2023. A consistent volume-of-fluid approach for direct numerical simulation of the aerodynamic breakup of a vaporizing drop. Computers & Fluids 254 105807.

Coupling with a geometric VOF method

Velocity extension

- Always true in pure gas cells ($H_{(i,j)} = 0$)

$$\frac{\Delta t}{\Delta} H_{(i,j)} \nabla_{\Delta} \cdot \boldsymbol{u} = 0$$

- Mass transfer redistribution [*,**]

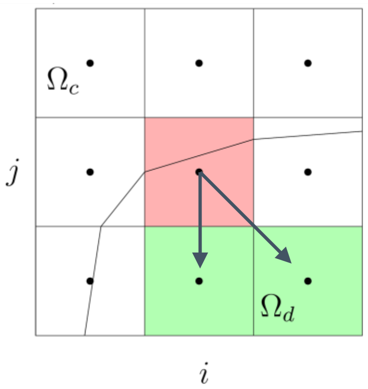

$$avg_{(i,j)} = \text{pure gas cells}\Big|_{3\times3}$$

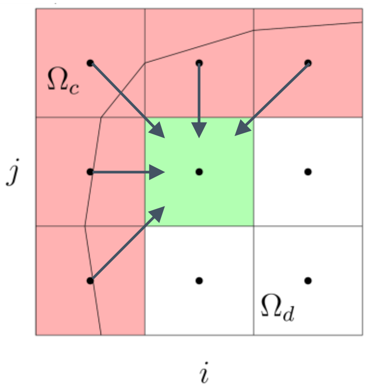

$$\dot{m}'_{(i,j)} = \sum_{3\times3} \frac{\dot{m}_{(l,k)}}{avg_{(l,k)}} A_{\Sigma(l,k)}$$

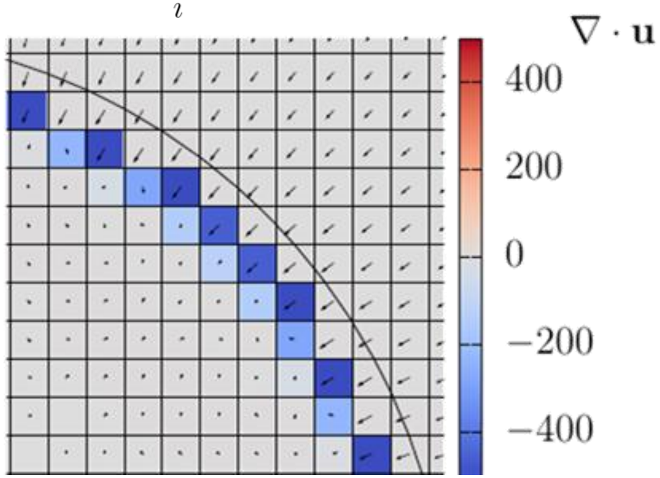

* Gennari, G., Jefferson-Loveday, R., Pickering, S. J., 2022. A phase-change model for diffusion-driven mass transfer problems in incompressible two-phase flows. Chem. Eng. Sci. 259 117791.
** Boyd, B., Ling, Y., 2023. A consistent volume-of-fluid approach for direct numerical simulation of the aerodynamic breakup of a vaporizing drop. Computers & Fluids 254 105807.

Validation

Velocity extension

- Bubble with constant mass transfer rate

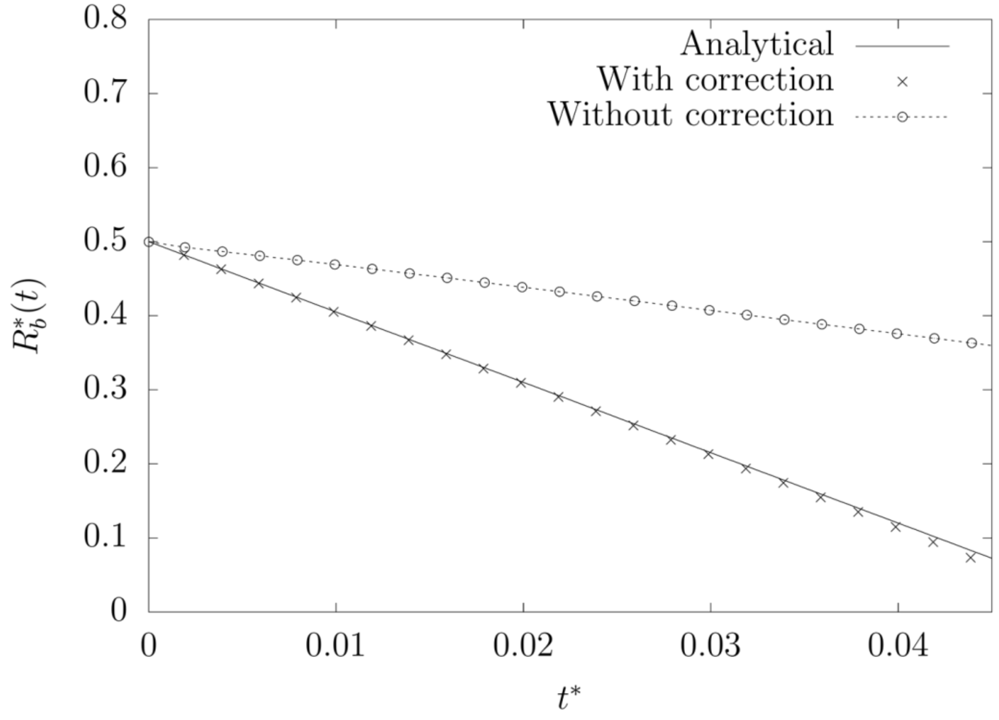

Validation

Velocity extension

- Bubble with constant mass transfer rate

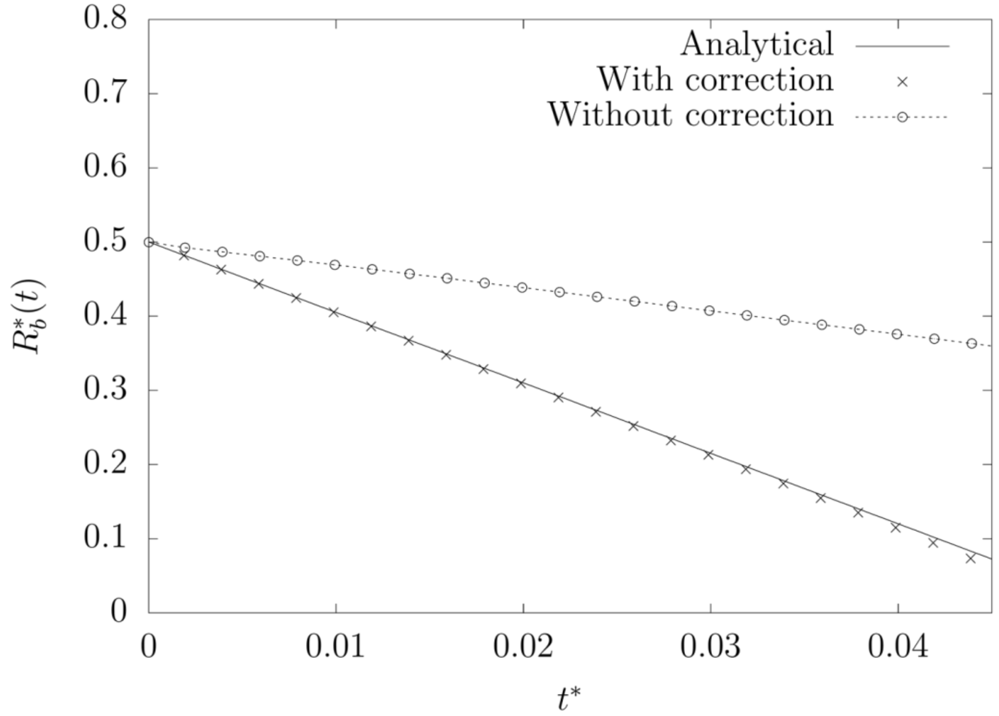

- With correction

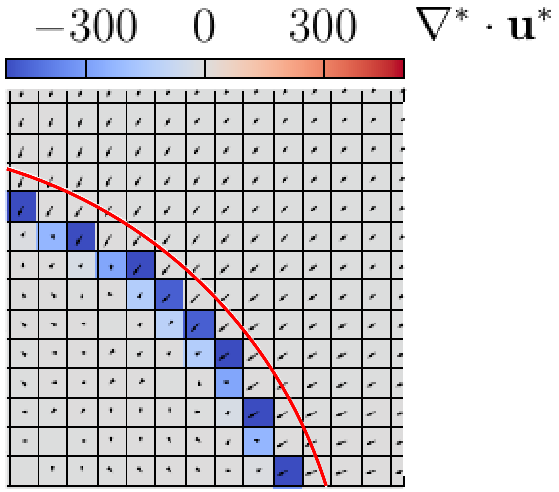

- Without correction

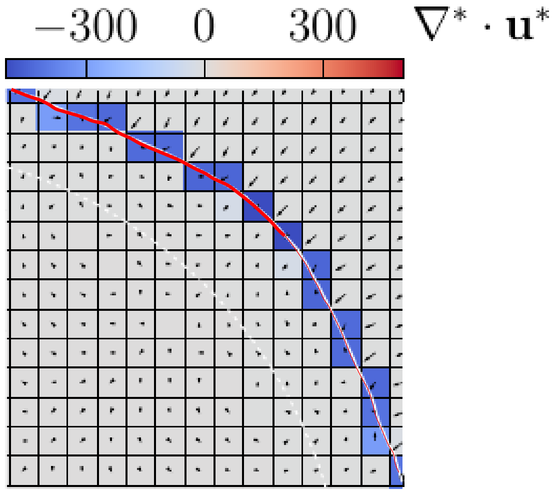

- More tests here [*]

* Gennari, G., Jefferson-Loveday, R., Pickering, S. J., 2022. A phase-change model for diffusion-driven mass transfer problems in incompressible two-phase flows. Chem. Eng. Sci. 259 117791.

Validation

Rising bubble at different Péclet numbers

- $$Sh = \frac{2}{\sqrt{\pi}}\left[1 - \frac{2}{3}\frac{1}{\left(1+0.09Re_b^{2/3}\right)^{3/4}}\right]^{1/2}\left(2.5+\sqrt{Pe}\right) \quad [*]$$

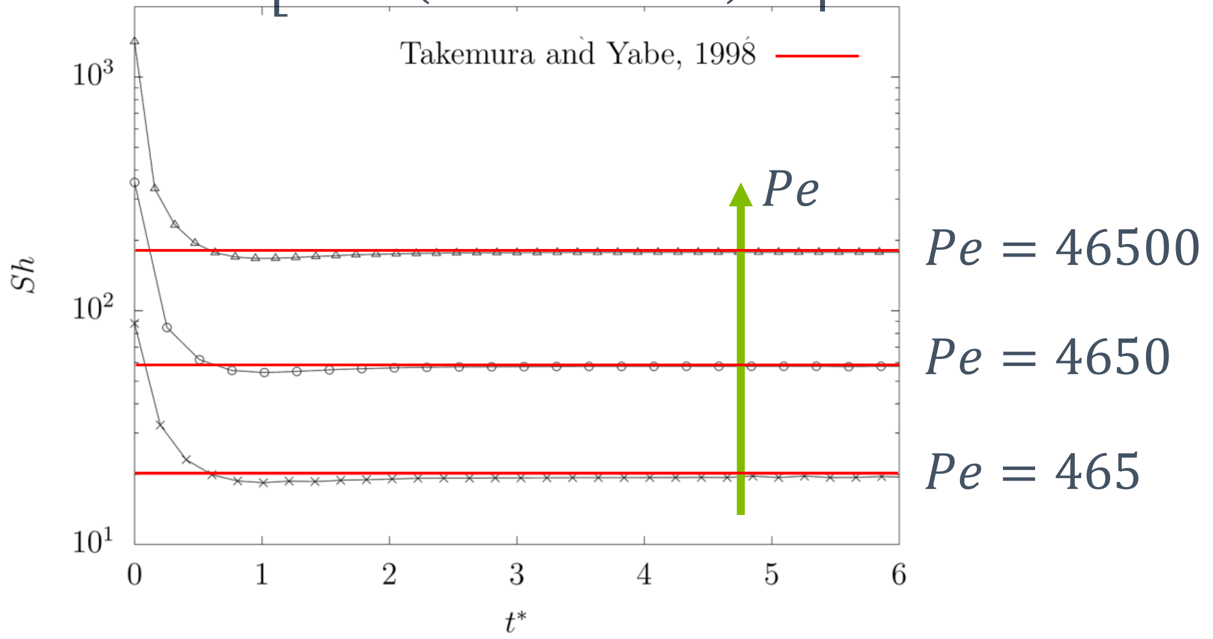

* Takemura, F., Yabe, A., 1998. Gas dissolution process of spherical rising gas bubbles. Chem. Eng. Sci. 53, 2691–2699.

Validation

Rising bubble at different Péclet numbers

- $Sh = \frac{2}{\sqrt{\pi}}\left[1 - \frac{2}{3}\frac{1}{\left(1+0.09Re_b^{2/3}\right)^{3/4}}\right]^{1/2}\left(2.5+\sqrt{Pe}\right)$ [*]

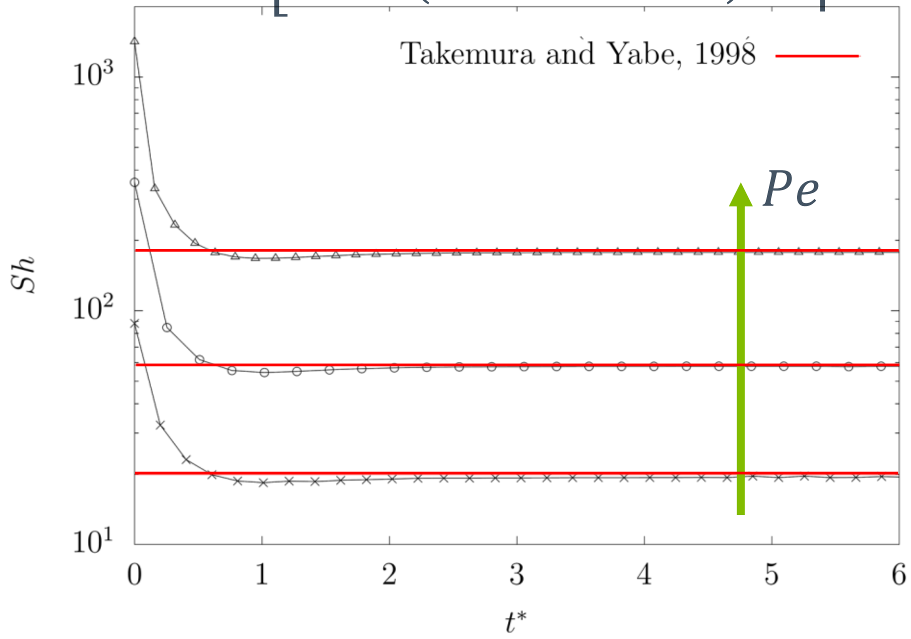

$Pe = 46500$

$Pe = 4650$

$Pe = 465$

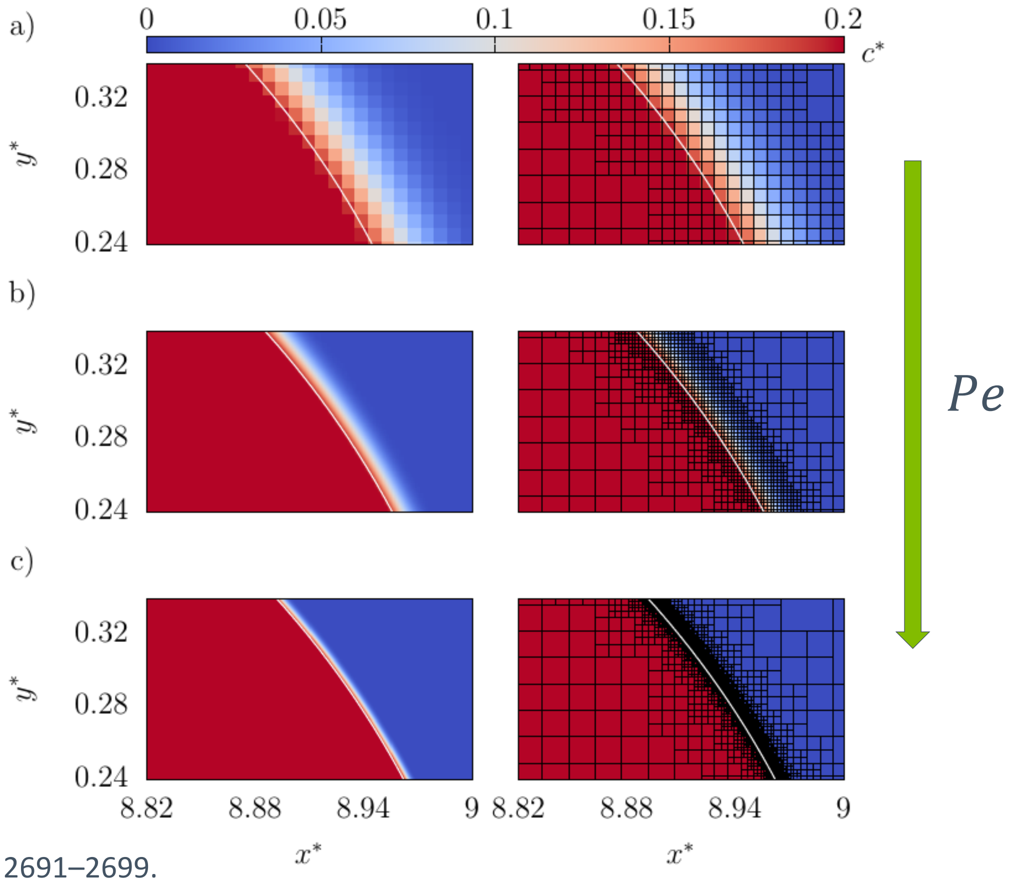

* Takemura, F., Yabe, A., 1998. Gas dissolution process of spherical rising gas bubbles. Chem. Eng. Sci. 53, 2691–2699.

Validation

Rising bubbles with different shapes

- Bubbles with generic shapes are corrected trough a shape factor: $Sr = {}^{A_\Sigma}/_{A_{sphere}}$

- Four cases [*]:

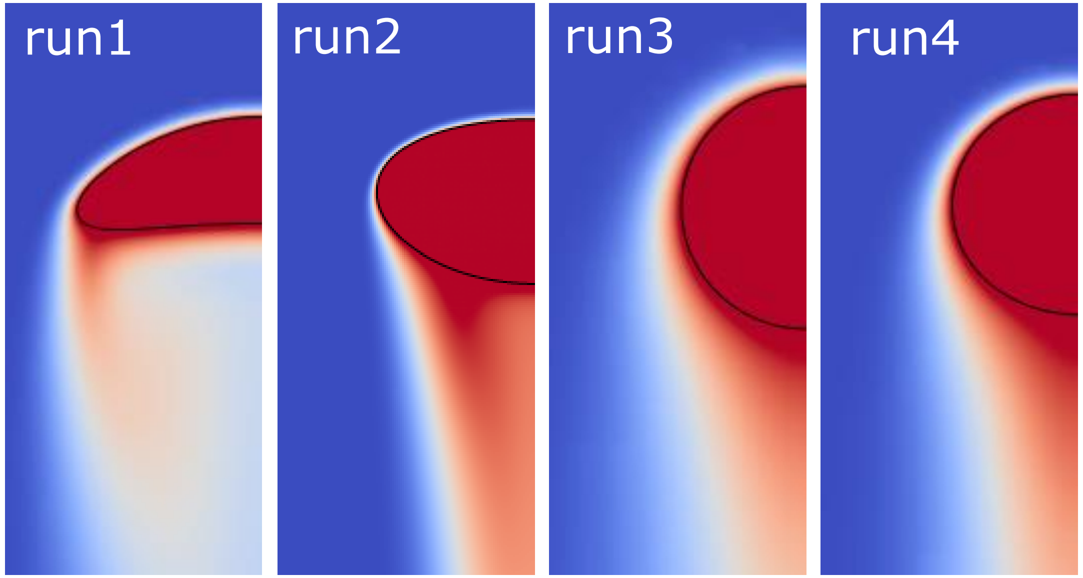

* Farsoiya, P., Magdelaine, Q., Antkowiak, A., Popinet, S., & Deike, L. (2023). Direct numerical simulations of bubble-mediated gas transfer and dissolution in quiescent and turbulent flows. *Journal of Fluid Mechanics, 954,* A29.

Validation

Rising bubbles with different shapes

- Bubbles with generic shapes are corrected trough a shape factor: $Sr = {}^{A_\Sigma}/_{A_{sphere}}$

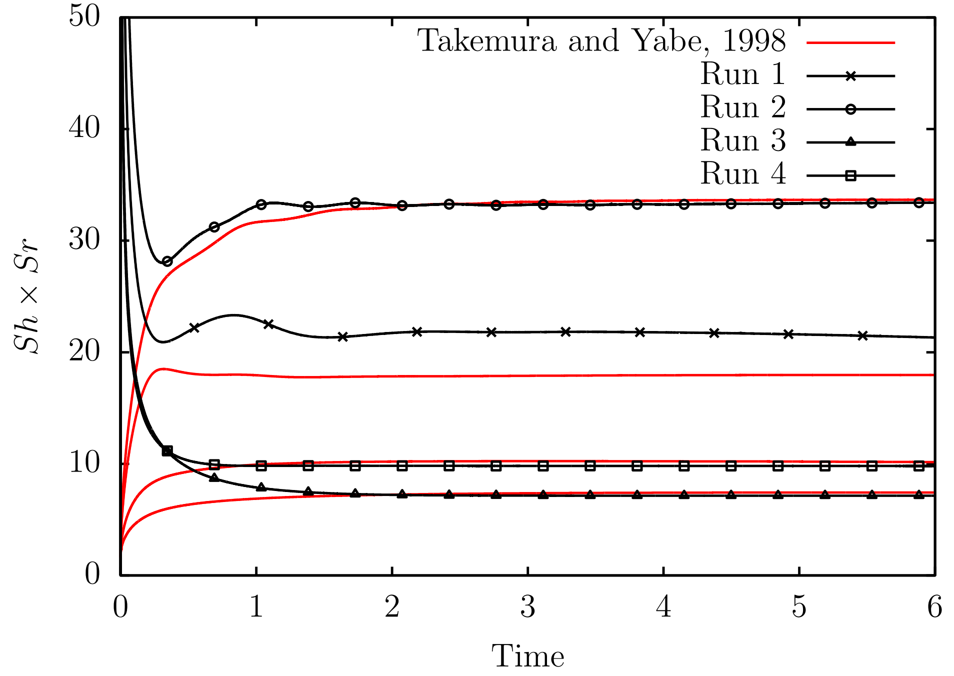

- Four cases [*]:

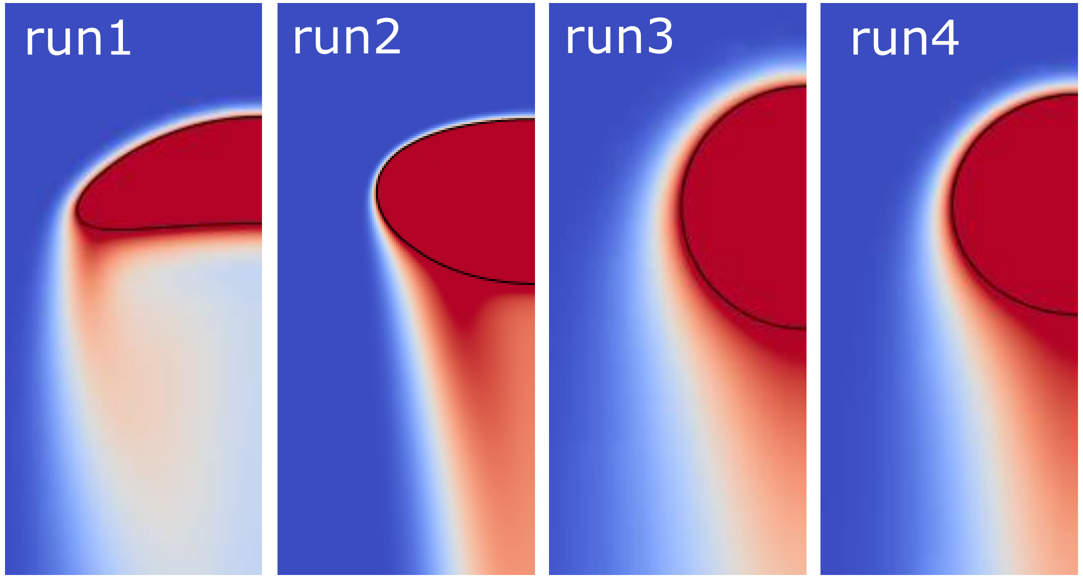

* Farsoiya, P., Magdelaine, Q., Antkowiak, A., Popinet, S., & Deike, L. (2023). Direct numerical simulations of bubble-mediated gas transfer and dissolution in quiescent and turbulent flows. *Journal of Fluid Mechanics, 954,* A29.

Taylor-Couette flow

Flow instability and Taylor vortices

- Vortices enhance the mixing within the reactor

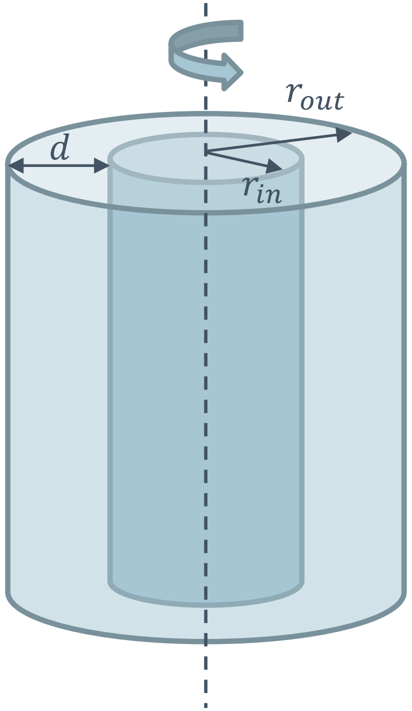

$$\eta = \frac{r_{in}}{r_{out}}$$

$$Re = \frac{\rho \Omega r_{in} d}{\mu}$$

Taylor-Couette flow

Flow instability and Taylor vortices

- Vortices enhance the mixing within the reactor

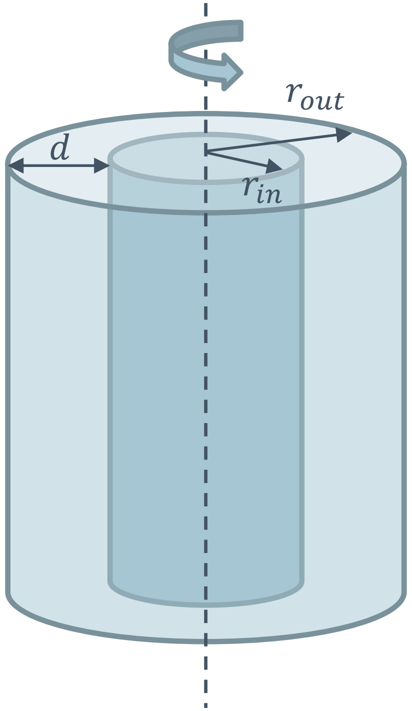

$$\eta = \frac{r_{in}}{r_{out}}$$

$$Re = \frac{\rho \Omega r_{in} d}{\mu}$$

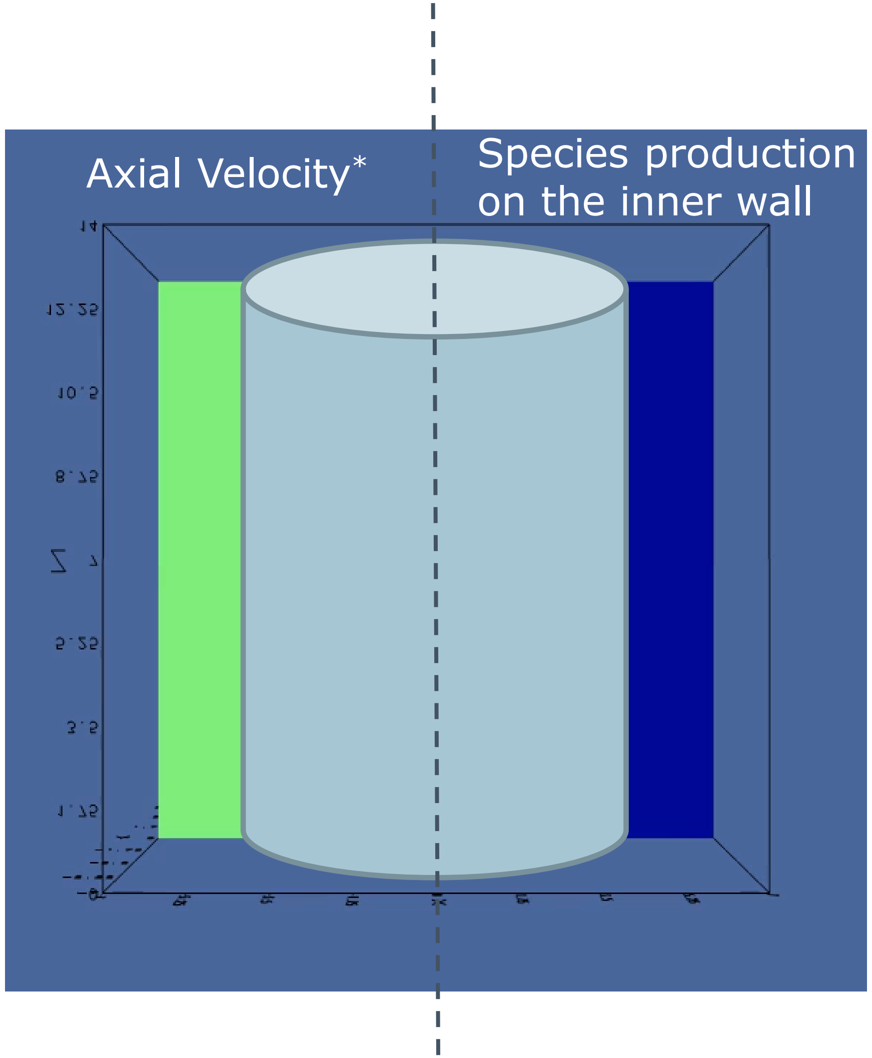

* $Re = 1000$

Taylor-Couette flow

Flow instability and Taylor vortices

- Vortices enhance the mixing within the reactor

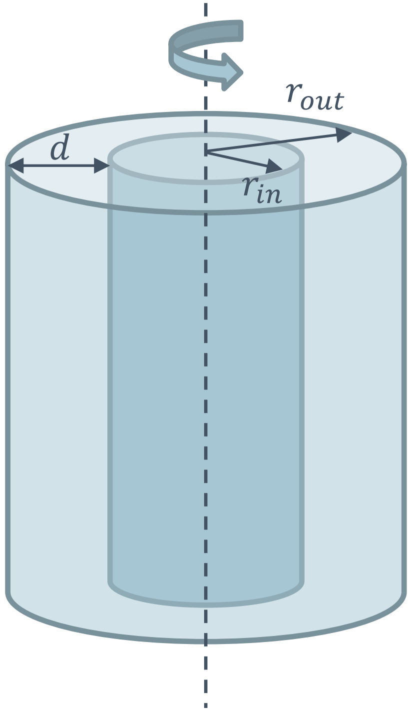

$$\eta = \frac{r_{in}}{r_{out}}$$

$$Re = \frac{\rho \Omega r_{in} d}{\mu}$$

Axial velocity

Outer wall

Inner wall

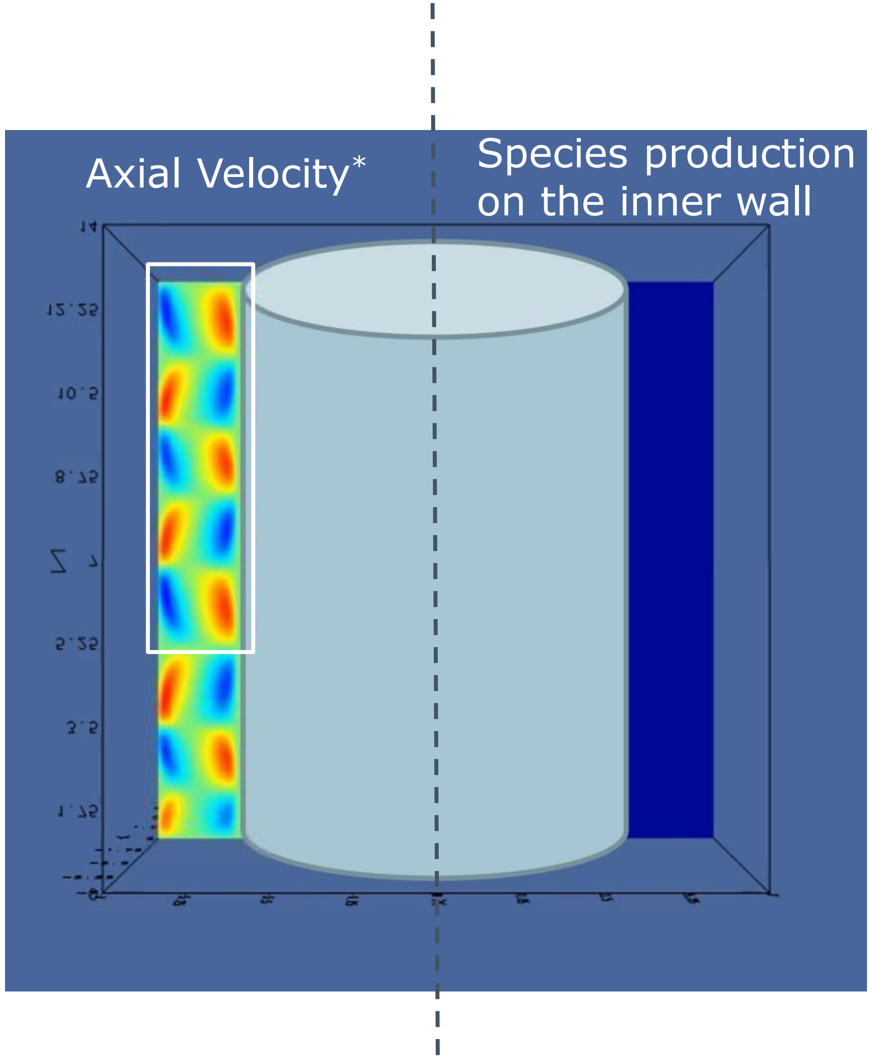

* $Re = 1000$

Taylor-Couette flow

Flow instability and Taylor vortices

- Contours of **axial velocity** at different Reynolds
- Radius ratio $\eta = \frac{r_{in}}{r_{out}} = 0.5$
- Periodic top/bottom boundaries

Case	Re	Regime
a)	1000	Laminar
b)	3000	Turbulent
c)	5000	Turbulent

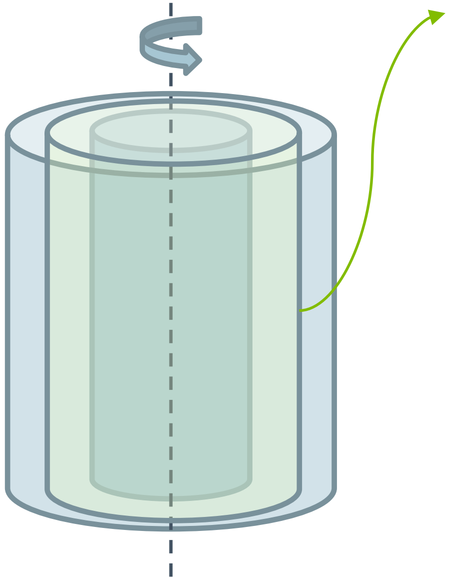

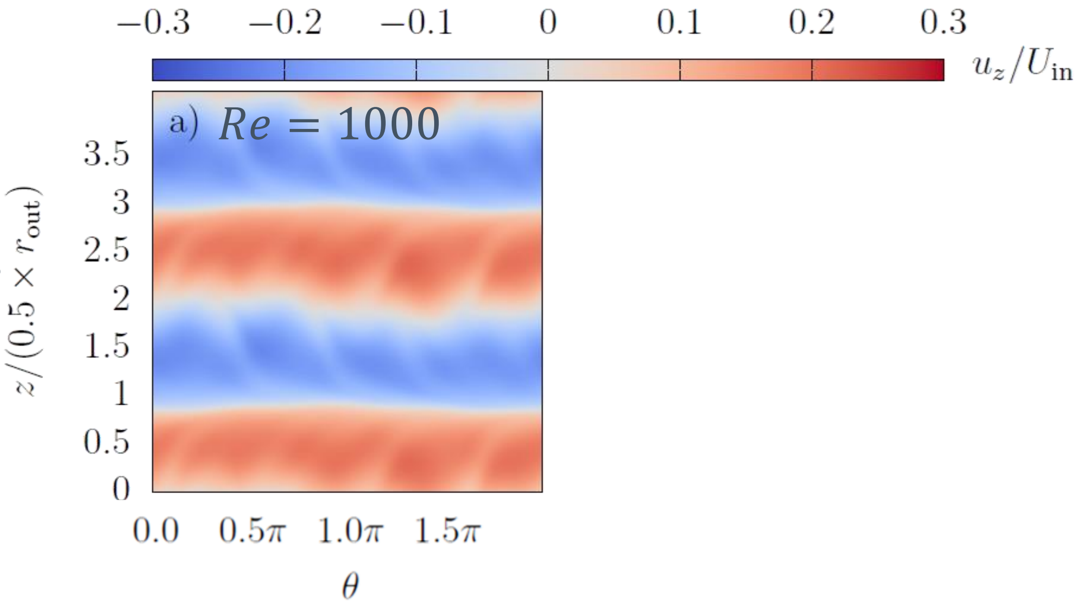

Taylor-Couette flow

Flow instability and Taylor vortices

- Contours of **axial velocity** at different Reynolds
- Radius ratio $\eta = \frac{r_{in}}{r_{out}} = 0.5$
- Periodic top/bottom boundaries

Case	Re	Regime
a)	1000	Laminar
b)	3000	Turbulent
c)	5000	Turbulent

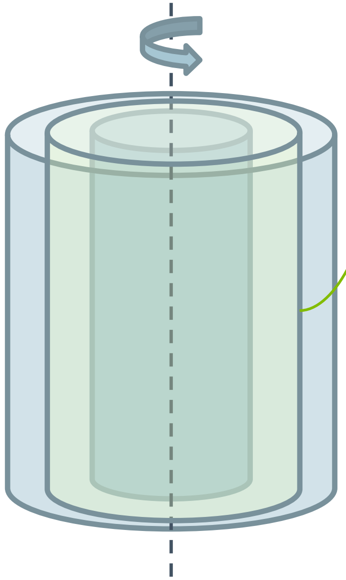

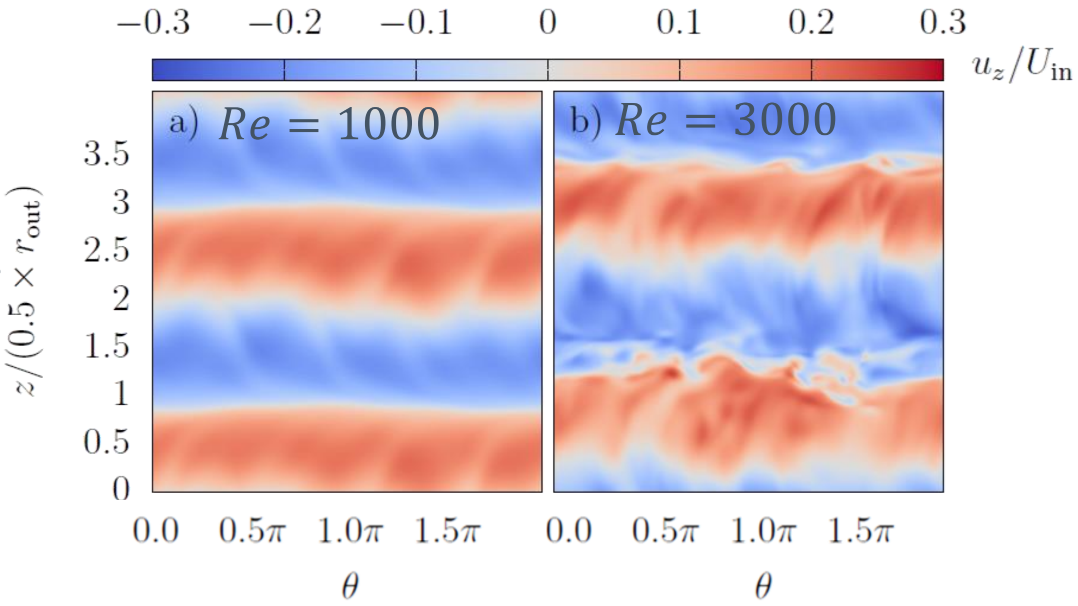

Taylor-Couette flow

Flow instability and Taylor vortices

- Contours of **axial velocity** at different Reynolds
- Radius ratio $\eta = \frac{r_{in}}{r_{out}} = 0.5$
- Periodic top/bottom boundaries

Case	Re	Regime
a)	1000	Laminar
b)	3000	Turbulent
c)	5000	Turbulent

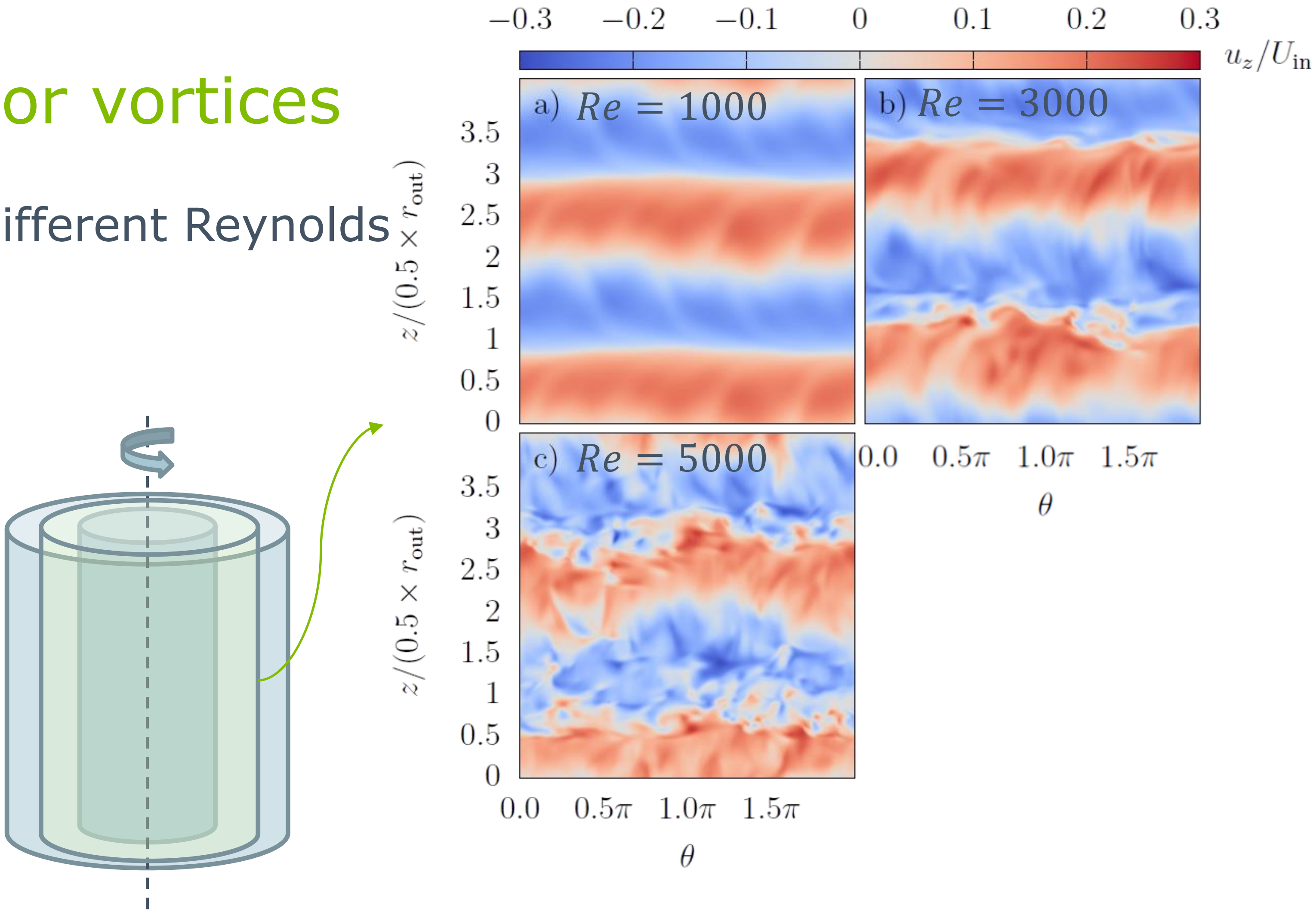

Taylor-Couette flow

Validation – Cylinder Torque

- Inner and Outer torques balance at equilibrium
- Non-dimensional torque:
  - $G_w = \frac{T_w}{\rho \nu^2 L_z}$

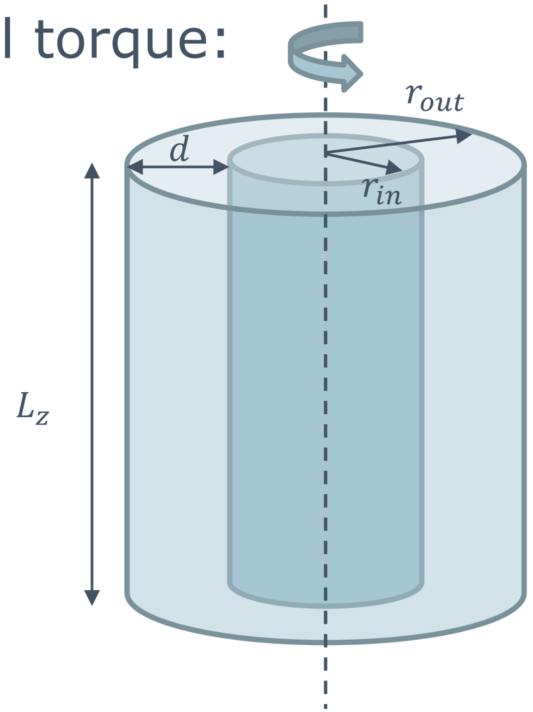

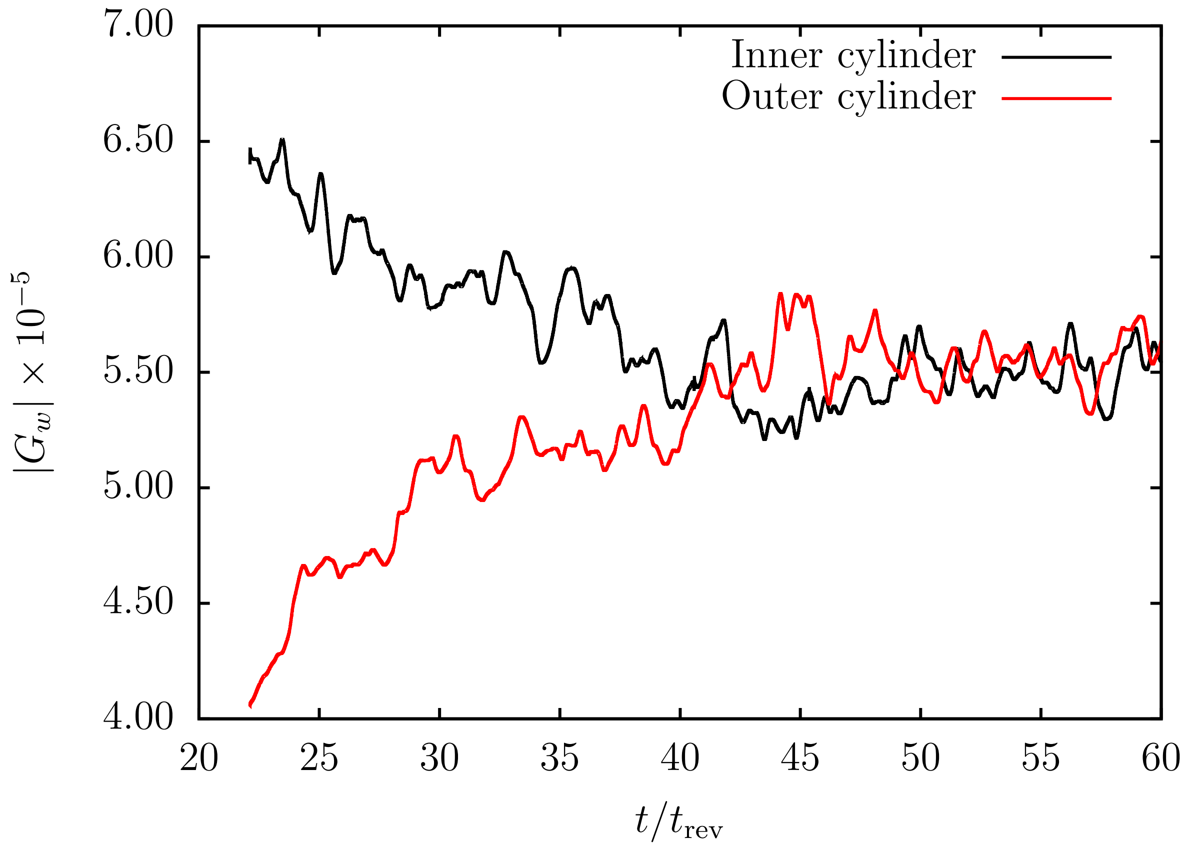

Taylor-Couette flow

Validation – Cylinder Torque

- Experimental Formula (Wendt, 1933 *):
  - $G_w = 1.45 \left[\frac{\eta^{3/2}}{(1-\eta)^{7/4}}\right] Re^{3/2}$

$$\eta = \frac{r_{in}}{r_{out}}$$

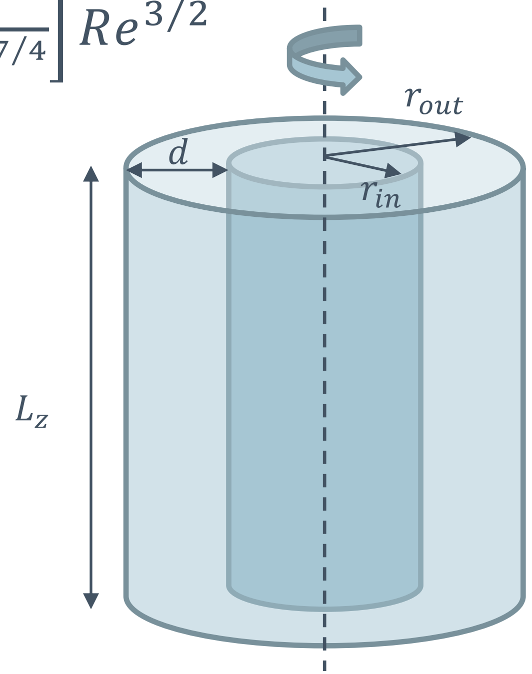

Non-dimensional Torque: $G_w = \frac{T_w}{\rho \nu^2 L_z}$

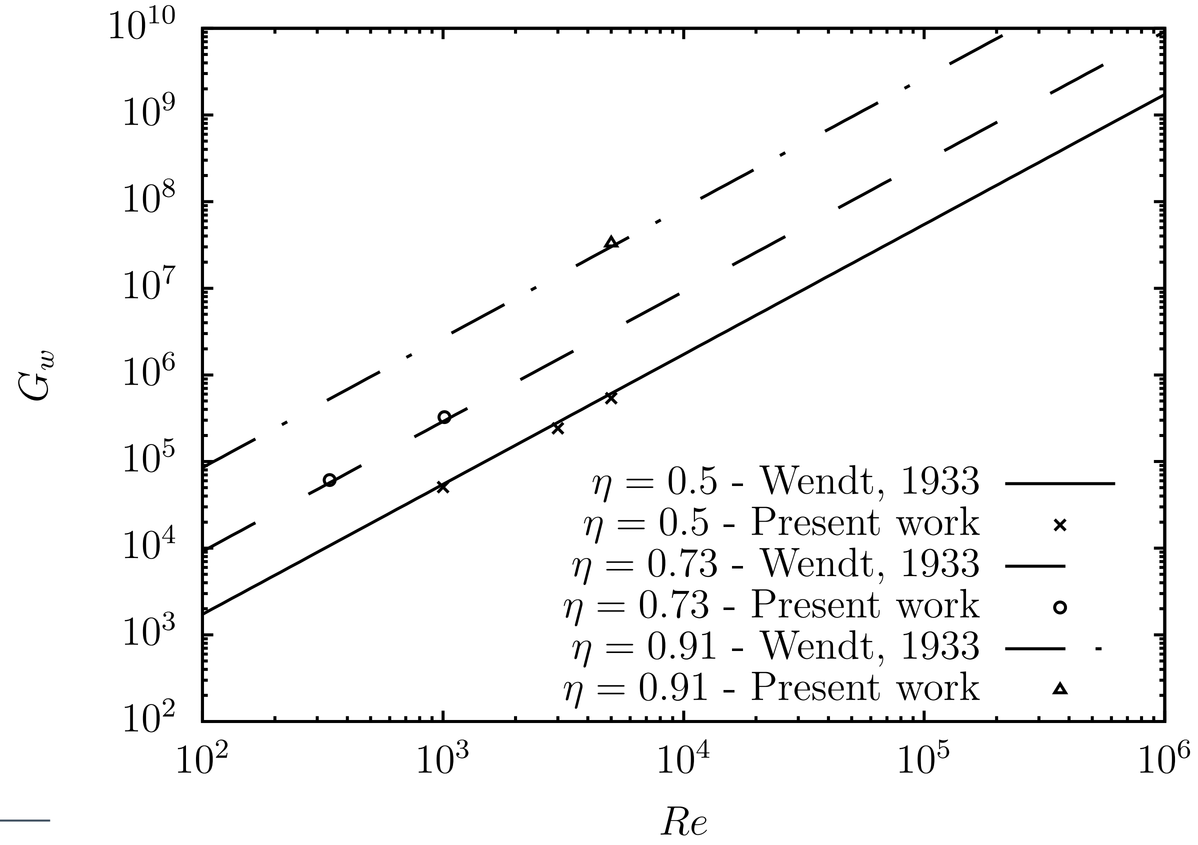

* Wendt, F. (1933). Turbulente strömungen zwischen zwei rotierenden konaxialen zylindern. *Ingenieur-Archiv, 4(6),* 577-595

Taylor-Couette flow

Validation – Velocity field

- Average azimuthal velocity

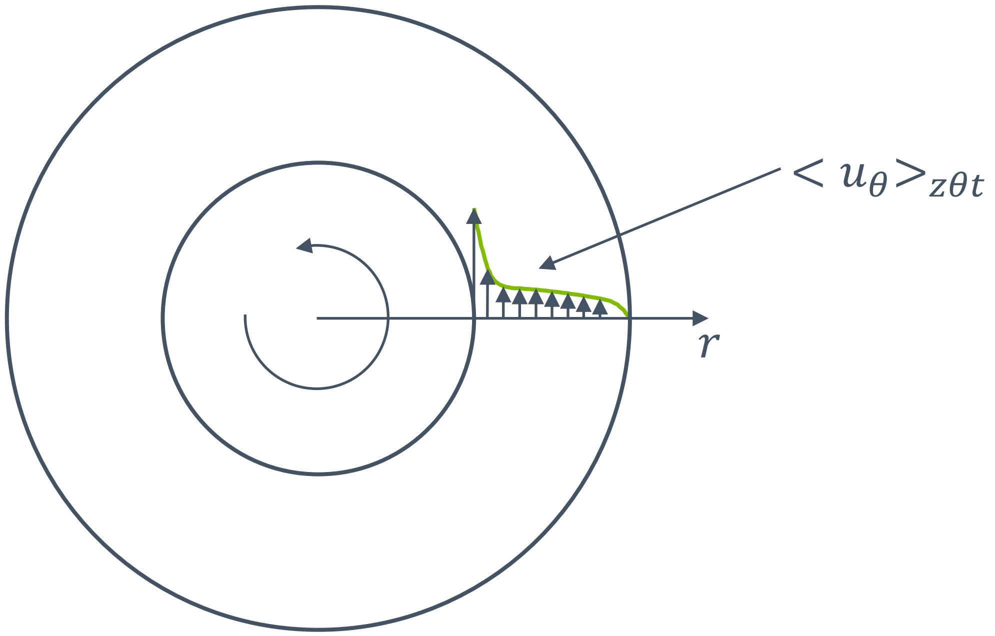

Taylor-Couette flow

Validation – Velocity field

- Average azimuthal velocity

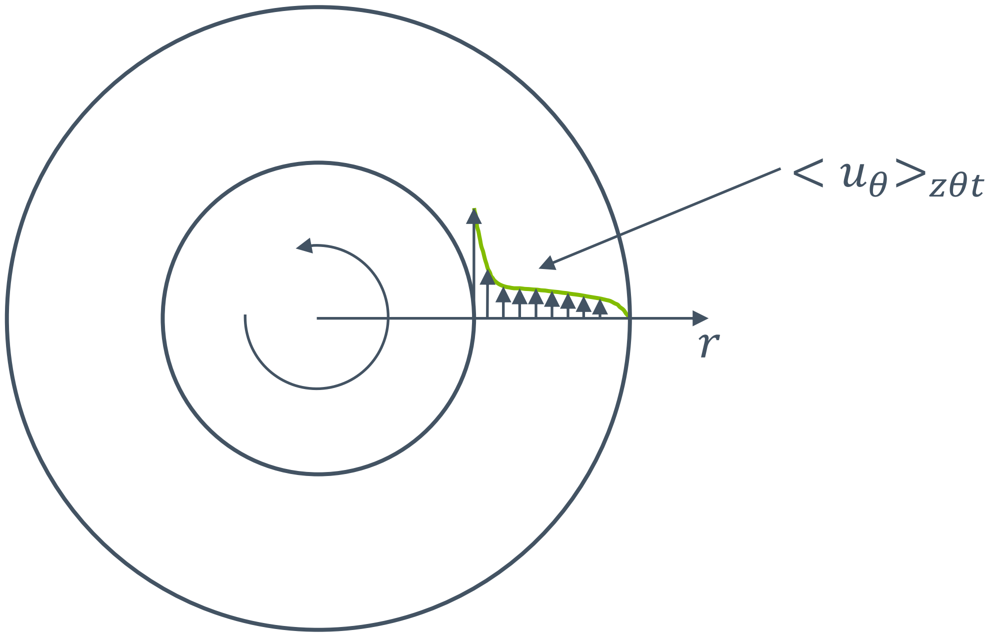

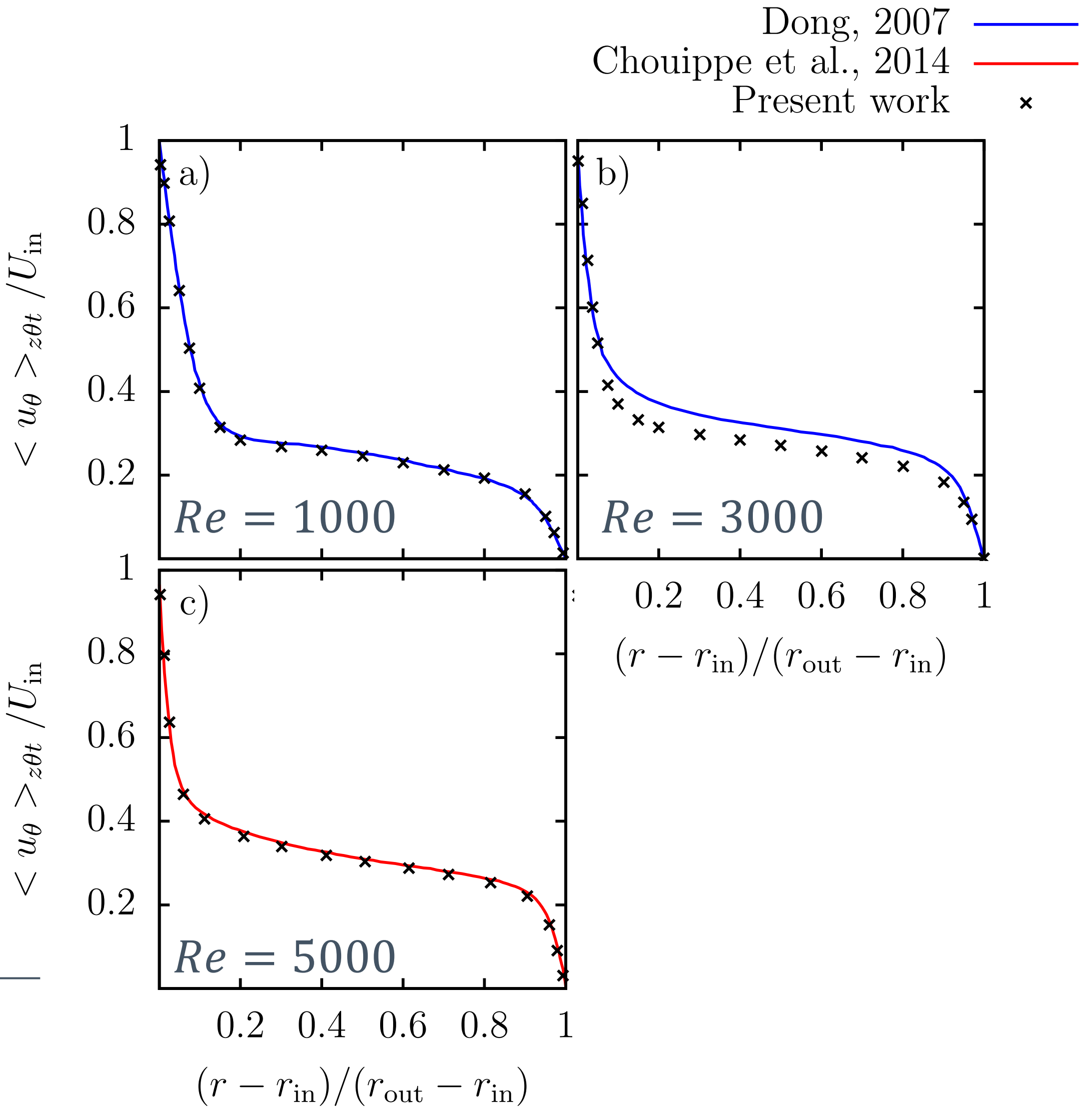

Chouippe, A., Climent, E., Legendre, D., & Gabillet, C. (2014). Numerical simulation of bubble dispersion in turbulent taylor-couette flow. Physics of Fluids, 26 (4), 043304.
Dong, S. (2007). Direct numerical simulation of turbulent taylor–couette flow. Journal of Fluid Mechanics, 587, 373–393

Taylor-Couette flow

Validation – Velocity field

- Average azimuthal velocity fluctuations
  - $u_\theta = < u_\theta > + u_\theta'$
- Typical two-peak profiles near the walls (channel flow)

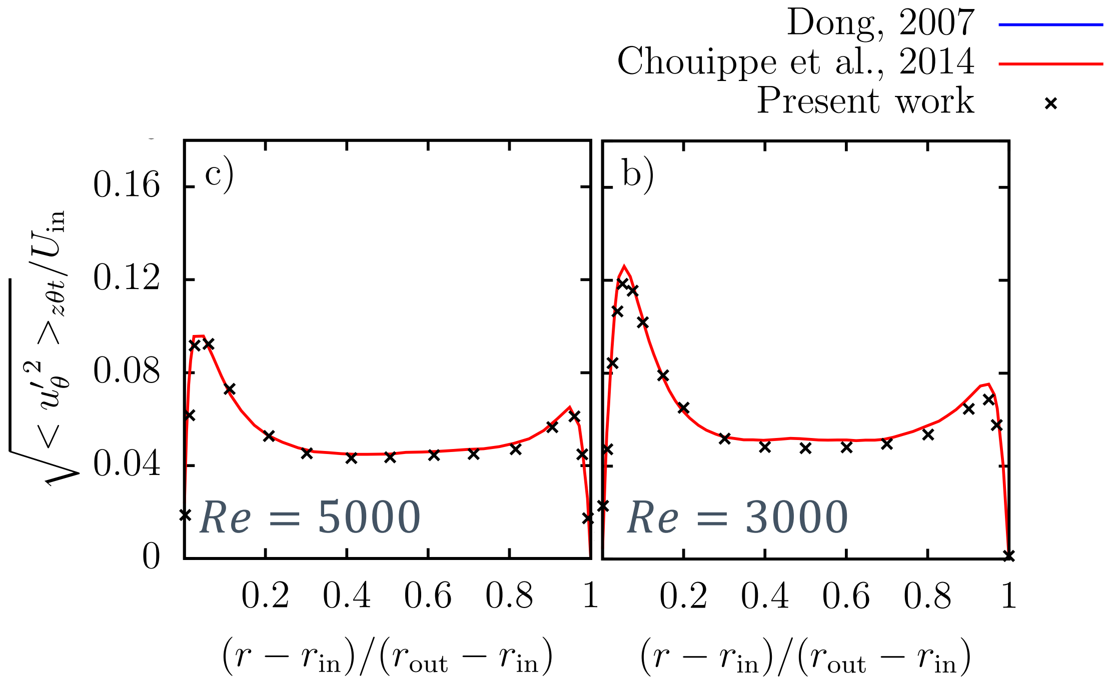

Chouippe, A., Climent, E., Legendre, D., & Gabillet, C. (2014). Numerical simulation of bubble dispersion in turbulent taylor-couette flow. Physics of Fluids, 26 (4), 043304.
Dong, S. (2007). Direct numerical simulation of turbulent taylor–couette flow. Journal of Fluid Mechanics, 587, 373–393

Mass transfer in Taylor-Couette flow
Simulation Setup

- A single bubble is let free to rise in an under-saturated liquid
- $Ga = 1050.7,\ Bo = 3.4,\ Sc = 0.458,\ {}^{\rho_c}/_{\rho_d} = 767.7,\ {}^{\mu_c}/_{\mu_d} = 52.2$

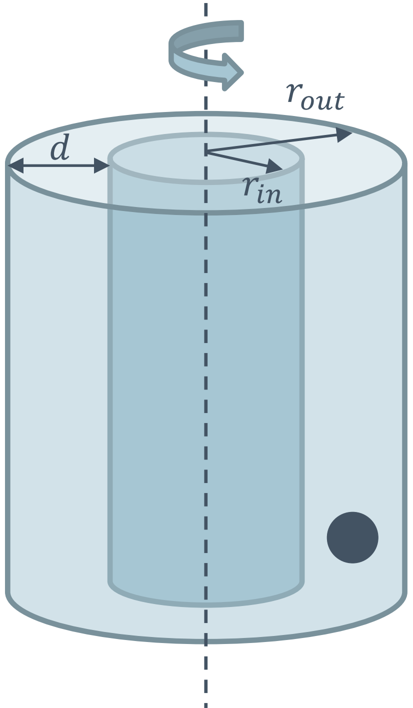

Case	Re	Regime	$D_b^{t=0}/d$	Cells/$D_b^{t=o}$	Gravity
a)	0	N/A	1/3	164	yes
b)	1000	Laminar	1/3	164	yes
c)	3000	Turbulent	1/3	164	yes
d)	5000	Turbulent	1/3	164	yes
e)	1000	Laminar	1/3	164	no
f)	3000	Turbulent	1/3	164	no
g)	5000	Turbulent	1/3	164	no

Mass transfer in Taylor-Couette flow

Iso-surfaces of dissolved gas

- Iso-surfaces of dissolved gas

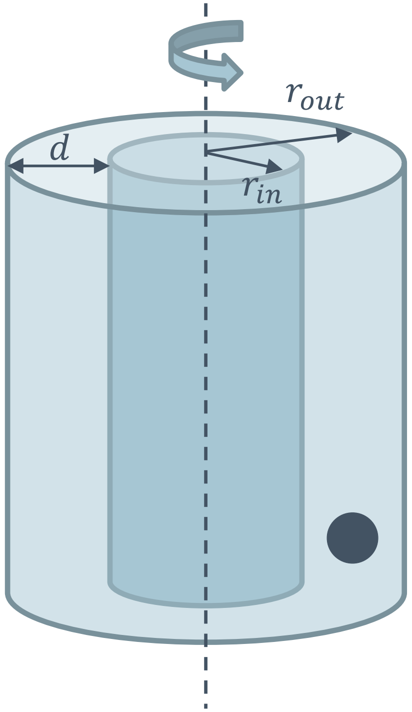

Case	Re	Regime
a)	0	N/A
b)	1000	Laminar
c)	3000	Turbulent
d)	5000	Turbulent

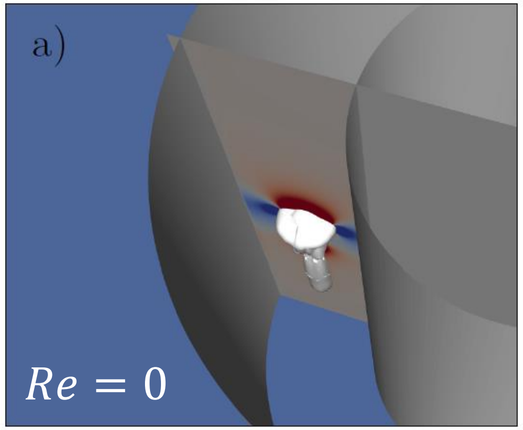

Mass transfer in Taylor-Couette flow

Iso-surfaces of dissolved gas

- Iso-surfaces of dissolved gas

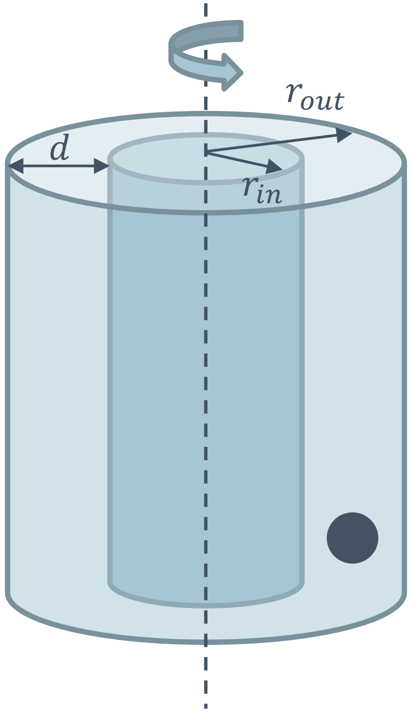

Case	Re	Regime
a)	0	N/A
b)	1000	Laminar
c)	3000	Turbulent
d)	5000	Turbulent

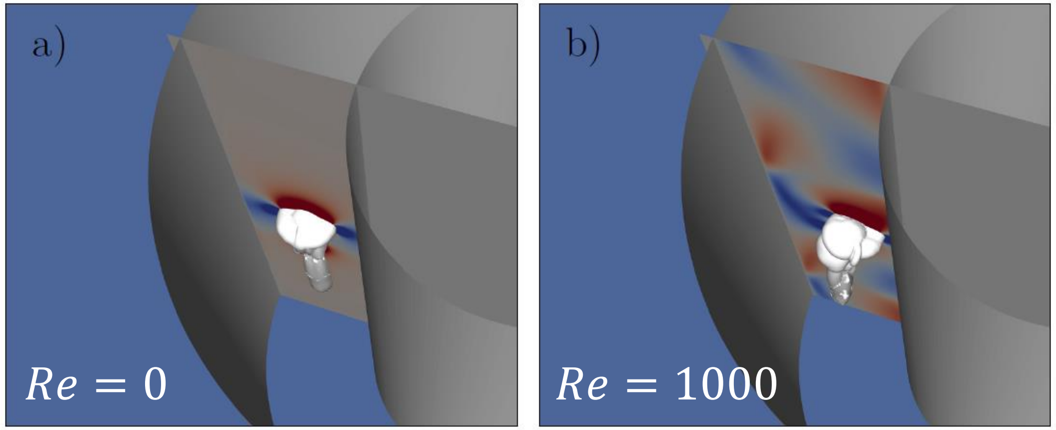

Mass transfer in Taylor-Couette flow

Iso-surfaces of dissolved gas

- Iso-surfaces of dissolved gas

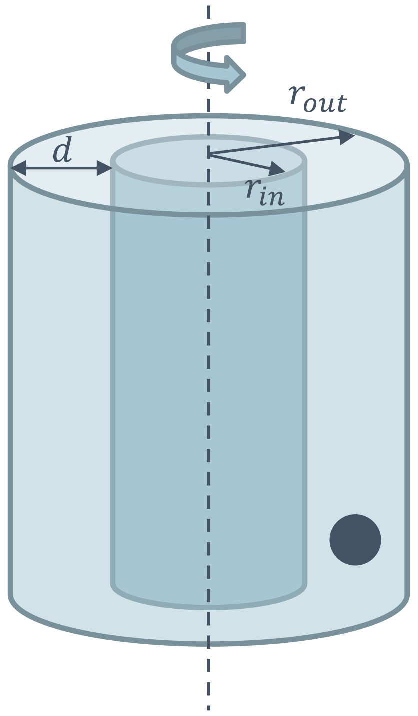

Case	Re	Regime
a)	0	N/A
b)	1000	Laminar
c)	3000	Turbulent
d)	5000	Turbulent

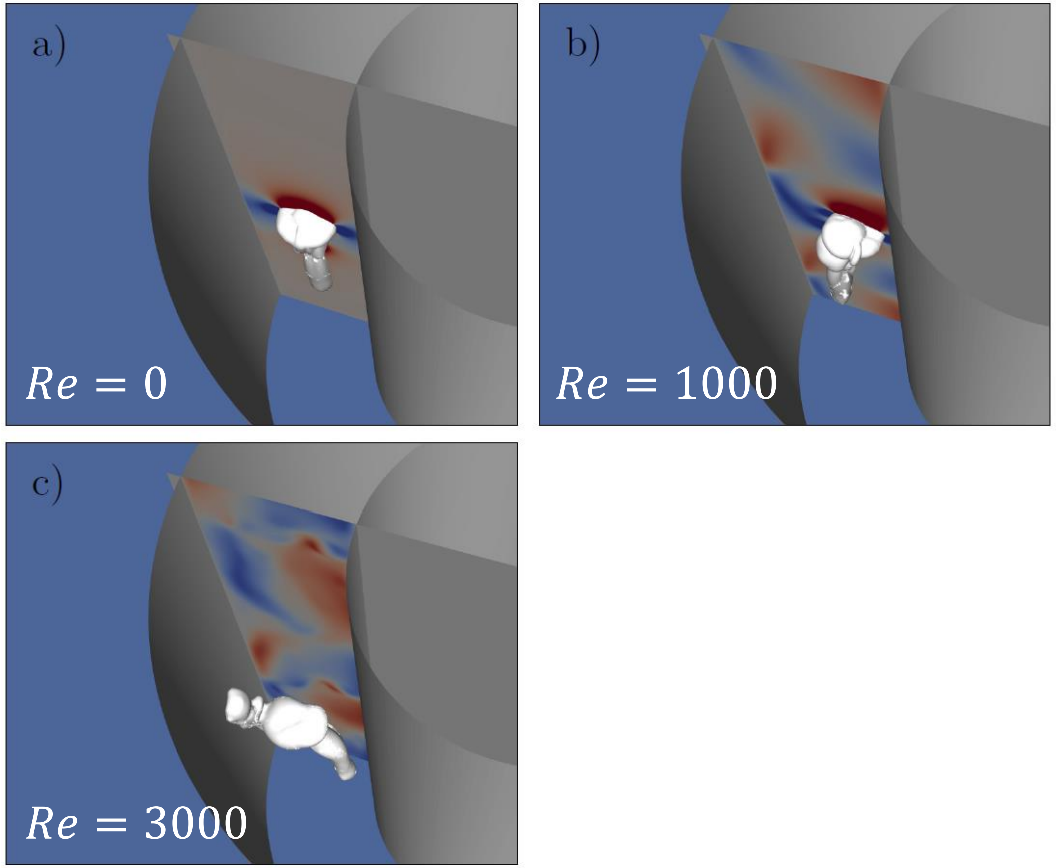

Mass transfer in Taylor-Couette flow

Iso-surfaces of dissolved gas

- Iso-surfaces of dissolved gas

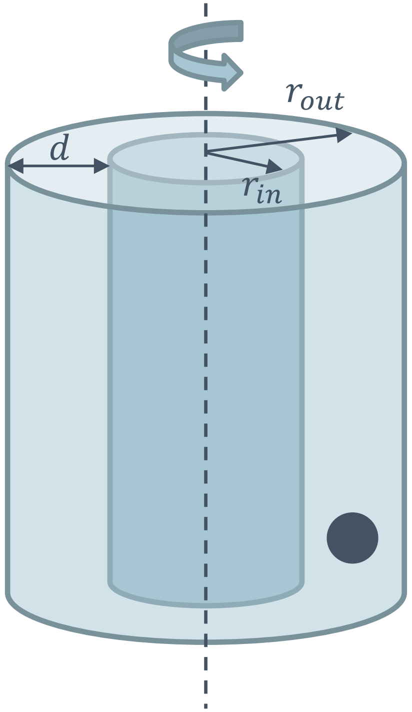

Case	Re	Regime
a)	0	N/A
b)	1000	Laminar
c)	3000	Turbulent
d)	5000	Turbulent

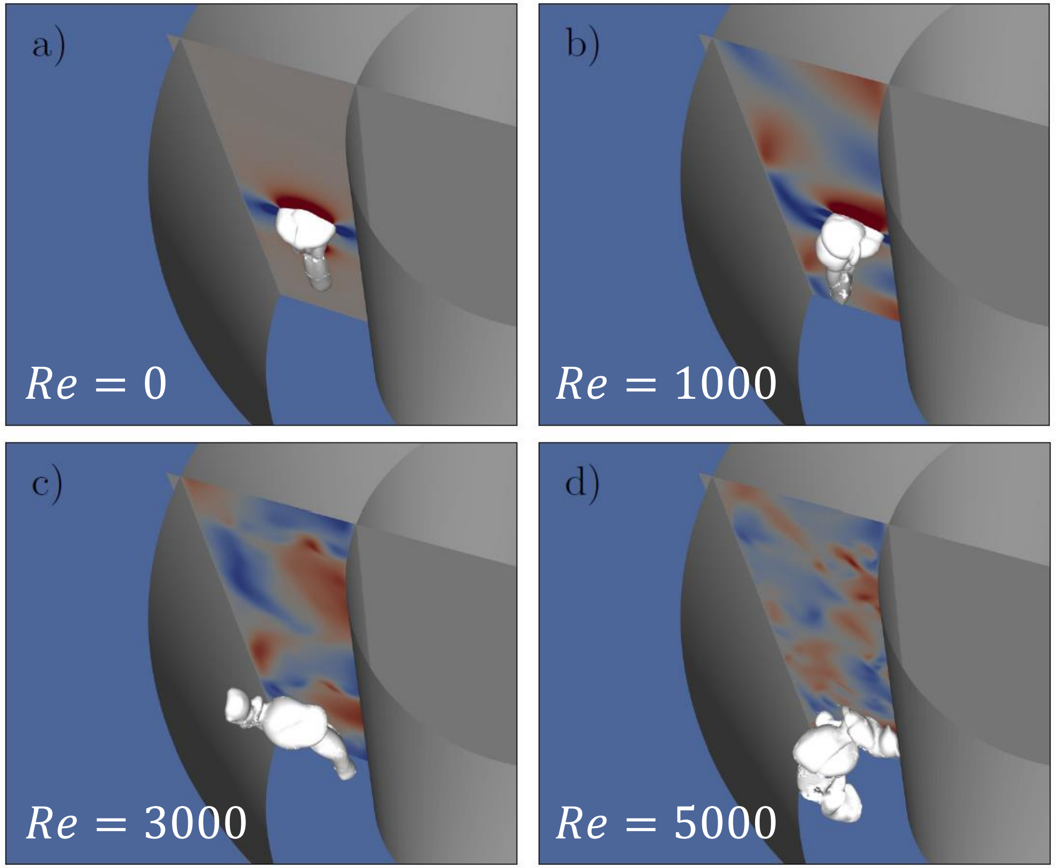

Mass transfer in Taylor-Couette flow

Volume dissolution

- Bubble initial diameter is $1/3$ of the gap
- Buoyancy and surface tension overcome the effect of the carrier flow on the dissolution rate.

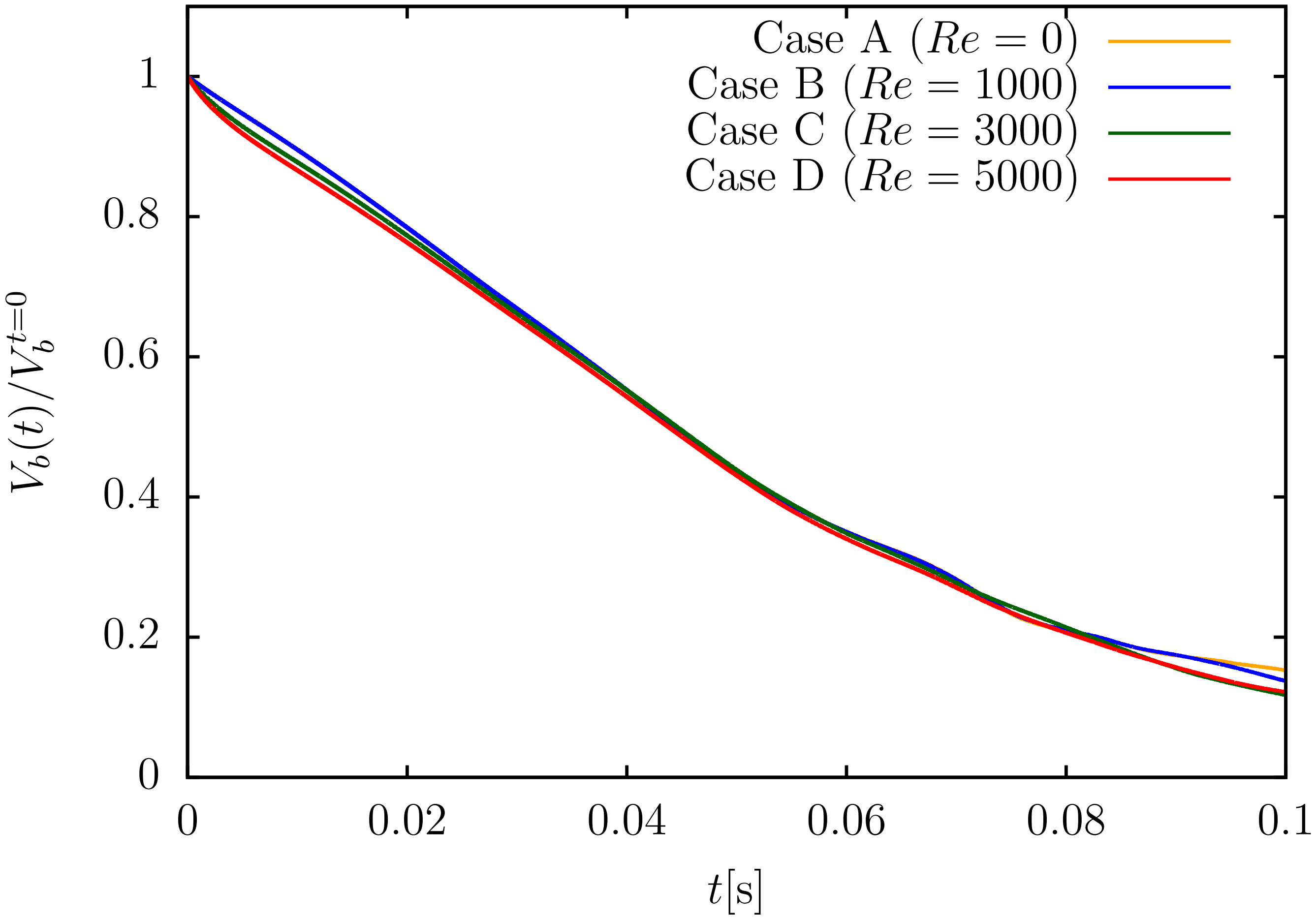

Mass transfer in Taylor-Couette flow

Sherwood numbers

- $Sh = \frac{k_m D_b}{D}, k_m = -\frac{\int_\Sigma \dot{m} dS}{A_\Sigma M \Delta c}$
- $Re_b = \frac{\rho_c U_b D_b}{\mu_c}$
- Sh and Re are generally related in bubbly flows driven by buoyancy.

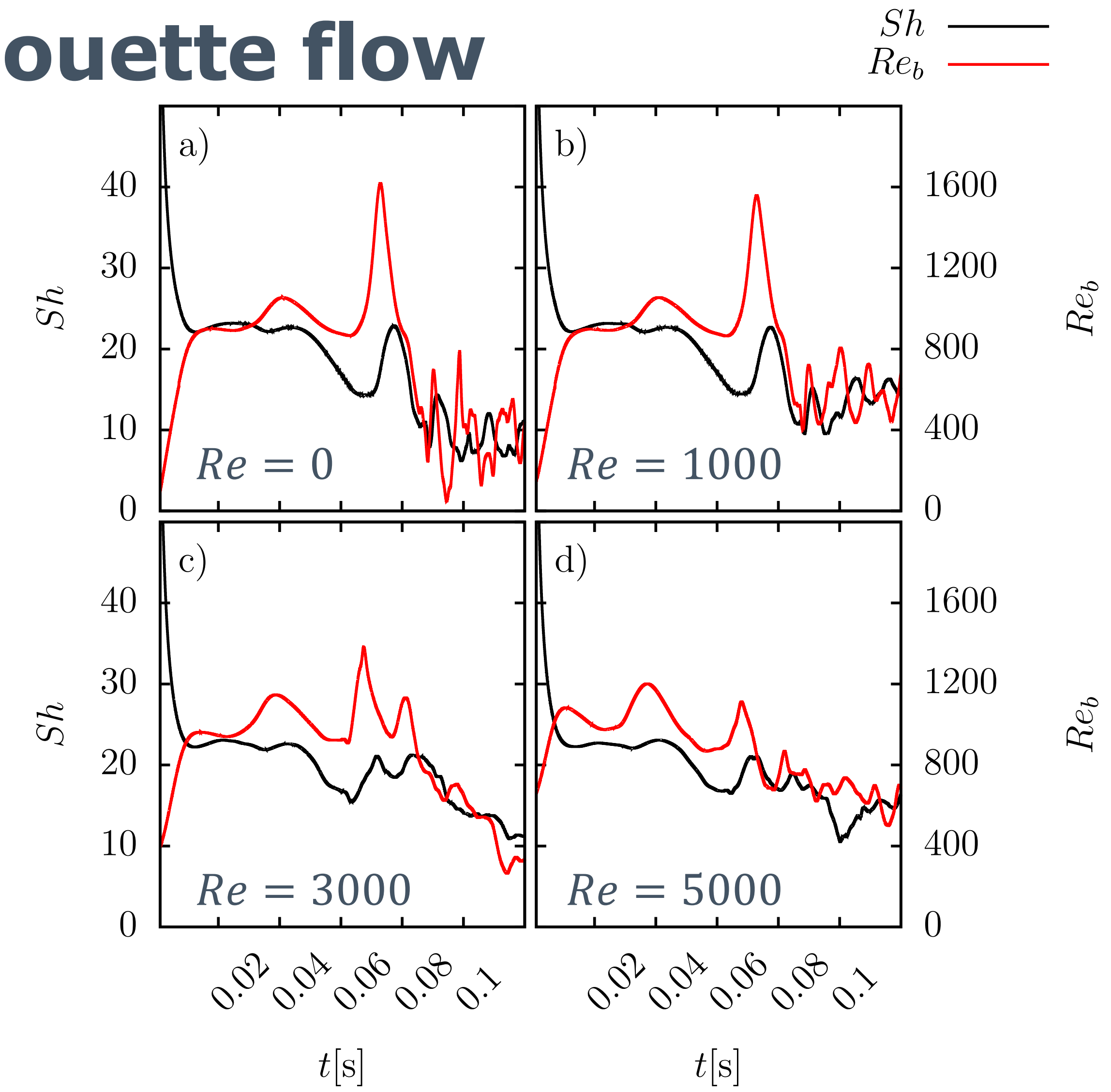

Mass transfer in Taylor-Couette flow

Sherwood numbers

- Typical behavior of the $Sh - Re$ curves suggests a comparison against common correlation formulae*:
  - $Sh = 2 + 0.651 \frac{Pe^{1.72}}{1+Pe^{1.22}}$ for $Re_b \rightarrow 0, Sc \rightarrow \infty$
  - $Sh = 2 + \frac{0.232Pe^{1.72}}{1+0.205Pe^{1.22}}$ for $Re_b \rightarrow \infty, Sc \rightarrow 0$

* Oellrich, L., Schmidt-Traub, H., & Brauer, H. (1973)

Mass transfer in Taylor-Couette flow

Sherwood numbers

- Typical behavior of the $Sh - Re$ curves suggests a comparison against common correlation formulae*:
  - $Sh = 2 + 0.651\frac{Pe^{1.72}}{1+Pe^{1.22}}$ for $Re_b \to 0, Sc \to \infty$
  - $Sh = 2 + \frac{0.232Pe^{1.72}}{1+0.205Pe^{1.22}}$ for $Re_b \to \infty, Sc \to 0$

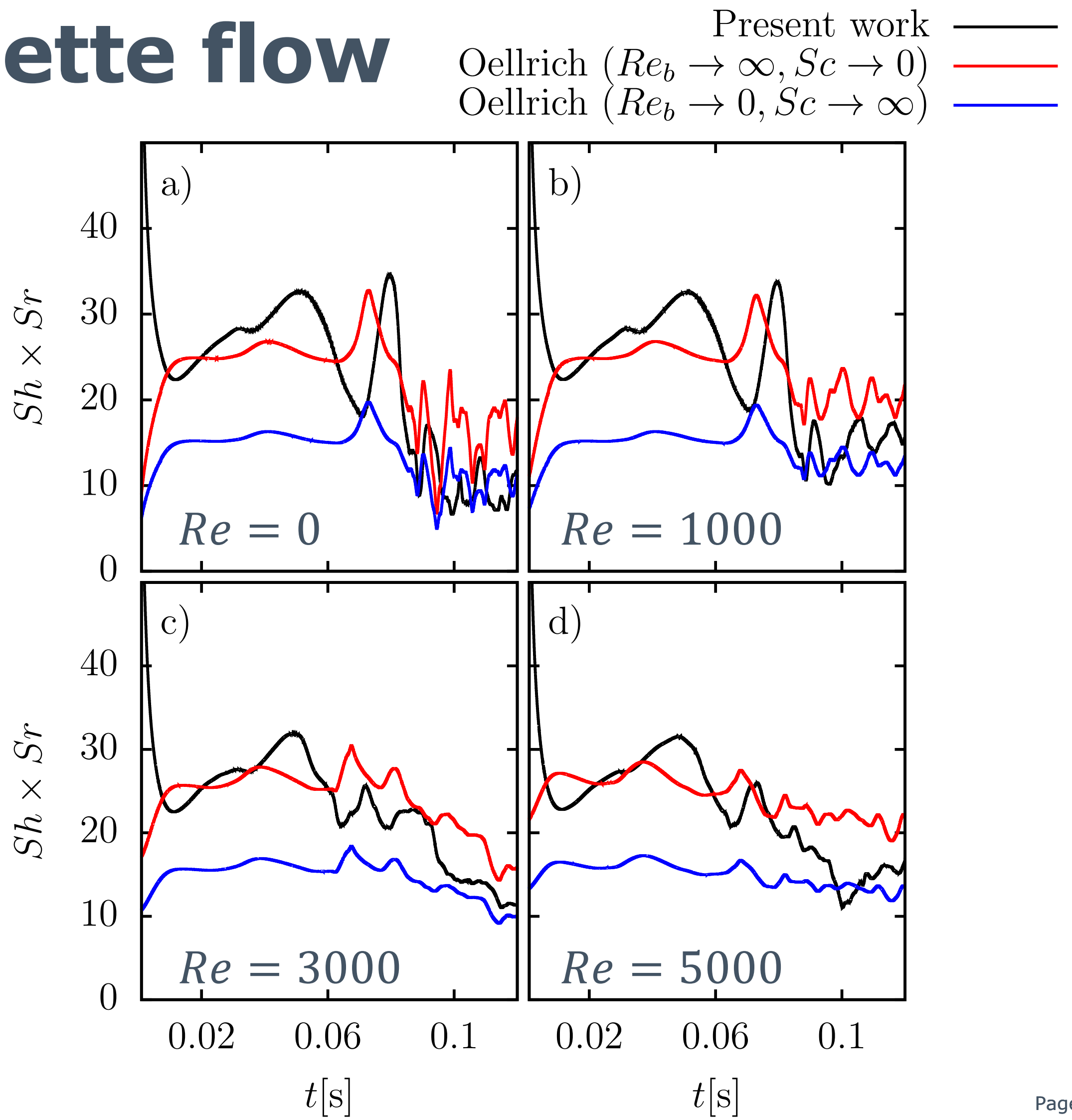

* Oellrich, L., Schmidt-Traub, H., & Brauer, H. (1973)

Mass transfer in Taylor-Couette flow

No gravity – trapped bubbles

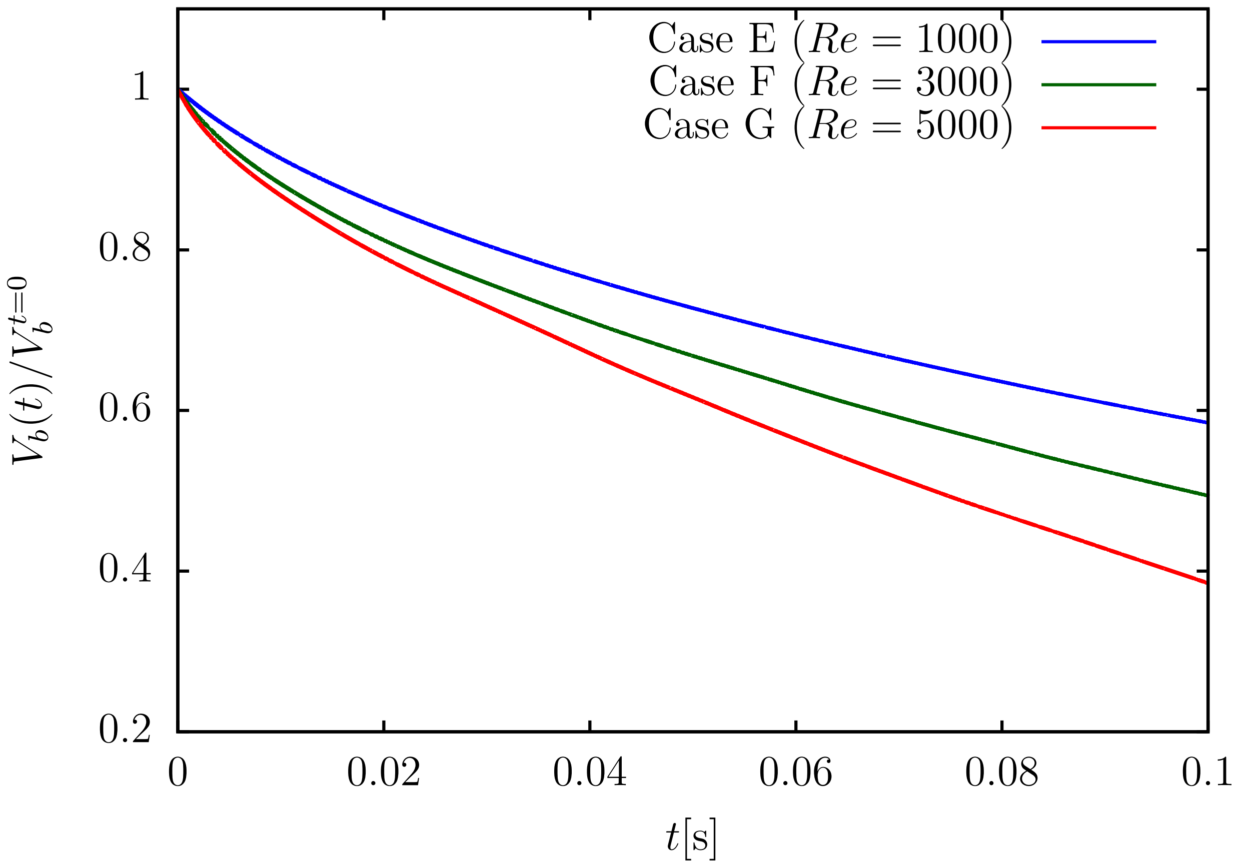

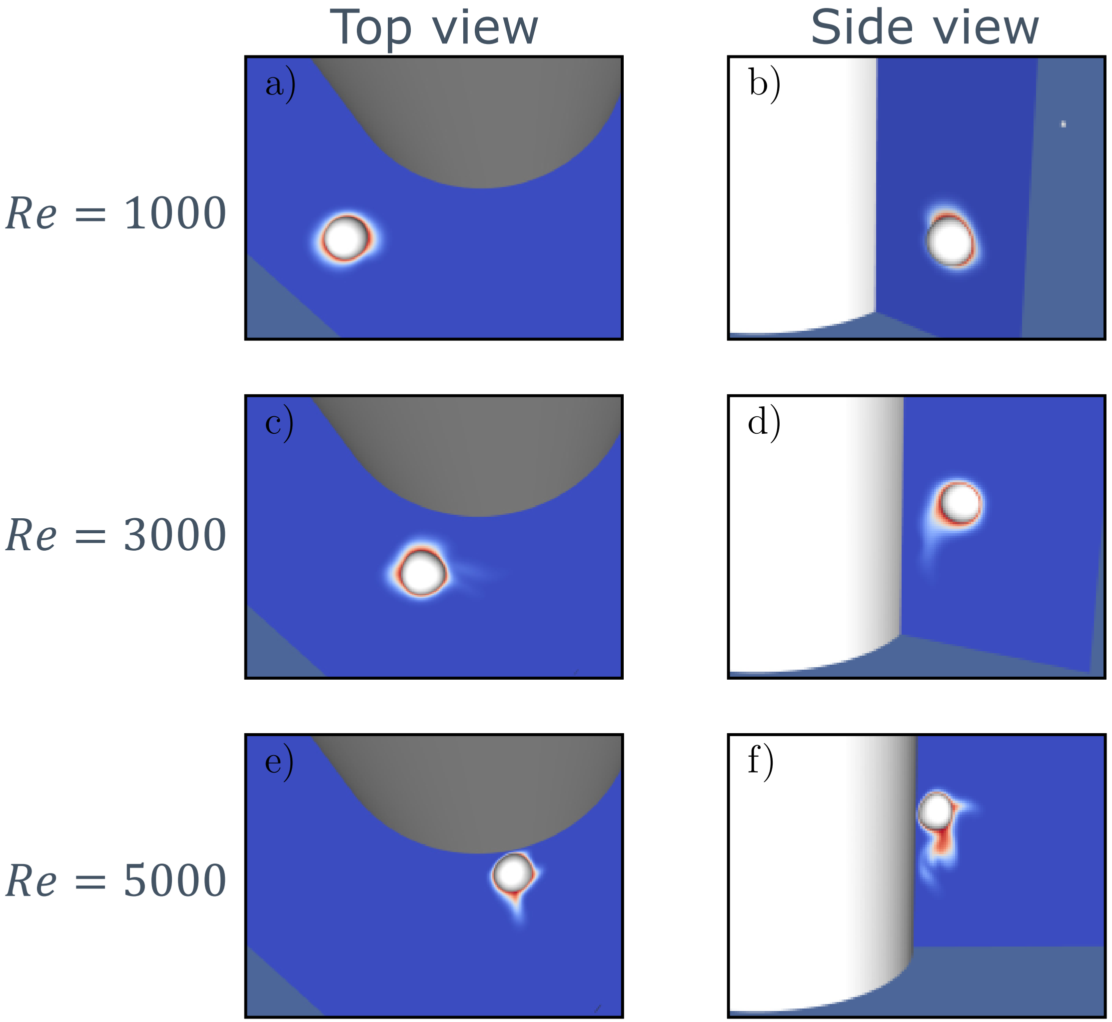

Taylor-Couette flow

Wake effect

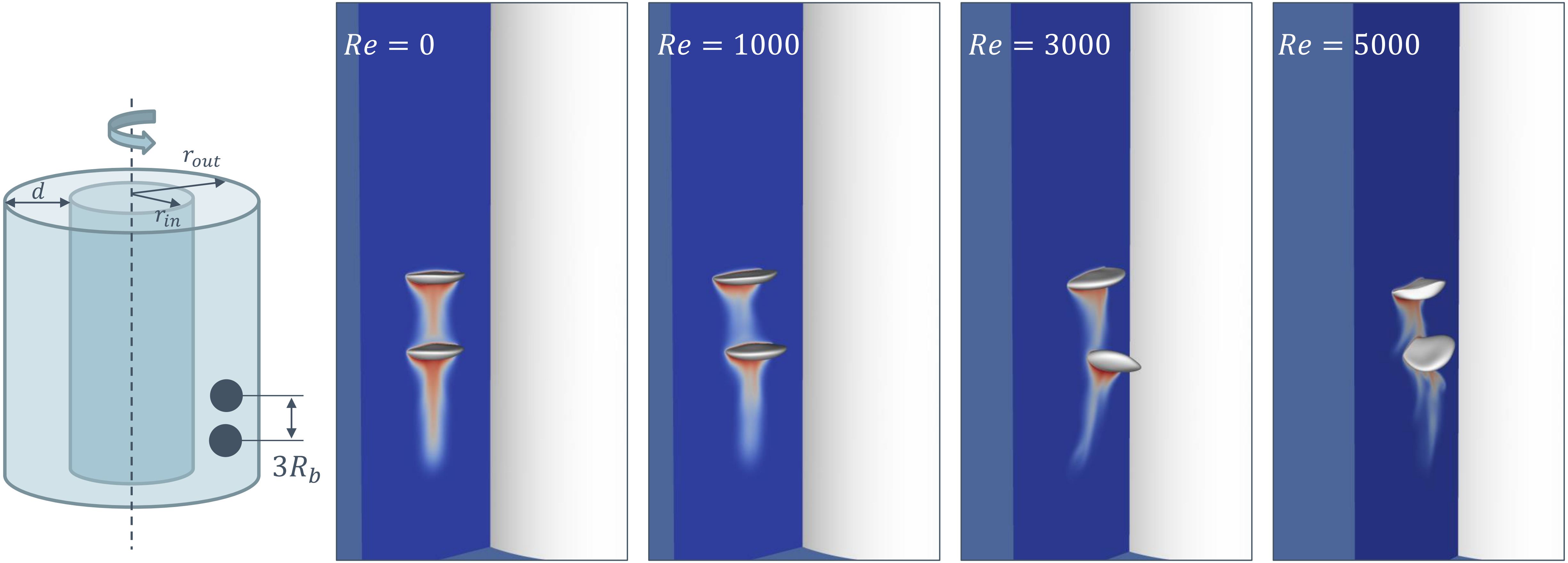

Taylor-Couette flow

Wake effect

- The top bubble behaves as if it were isolated
- The bottom bubble has a slower dissolution rate

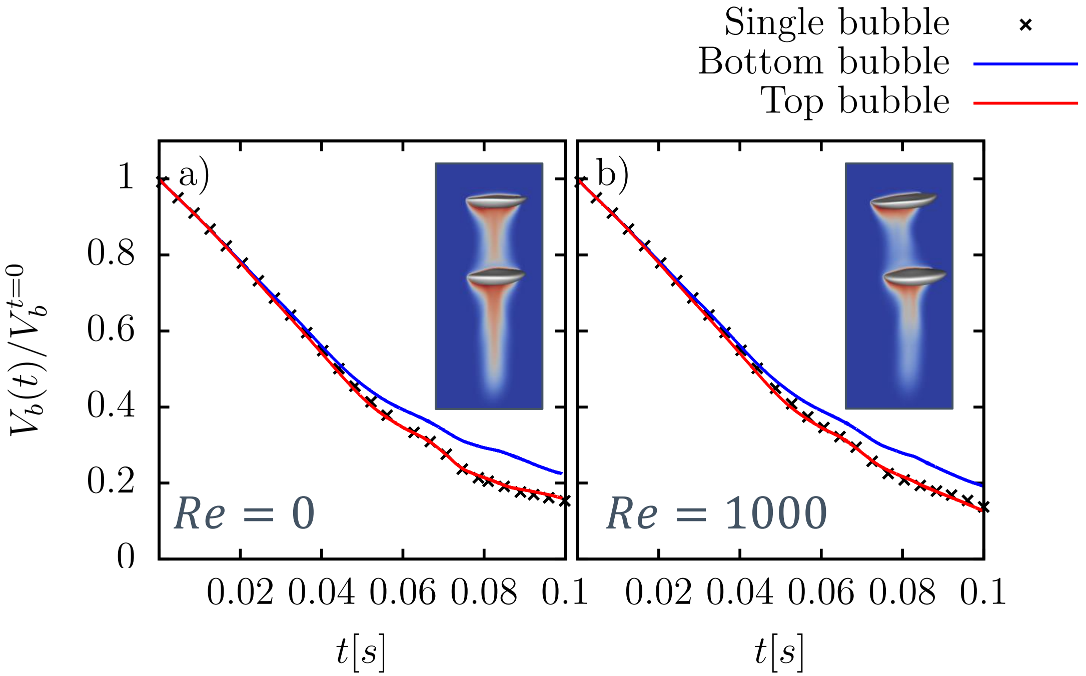

Taylor-Couette flow

Wake effect

- The top bubble behaves as if it were isolated
- The bottom bubble has a slower dissolution rate
- For larger rotating speed (and stronger Taylor vortices), top and bottom bubbles behave similarly

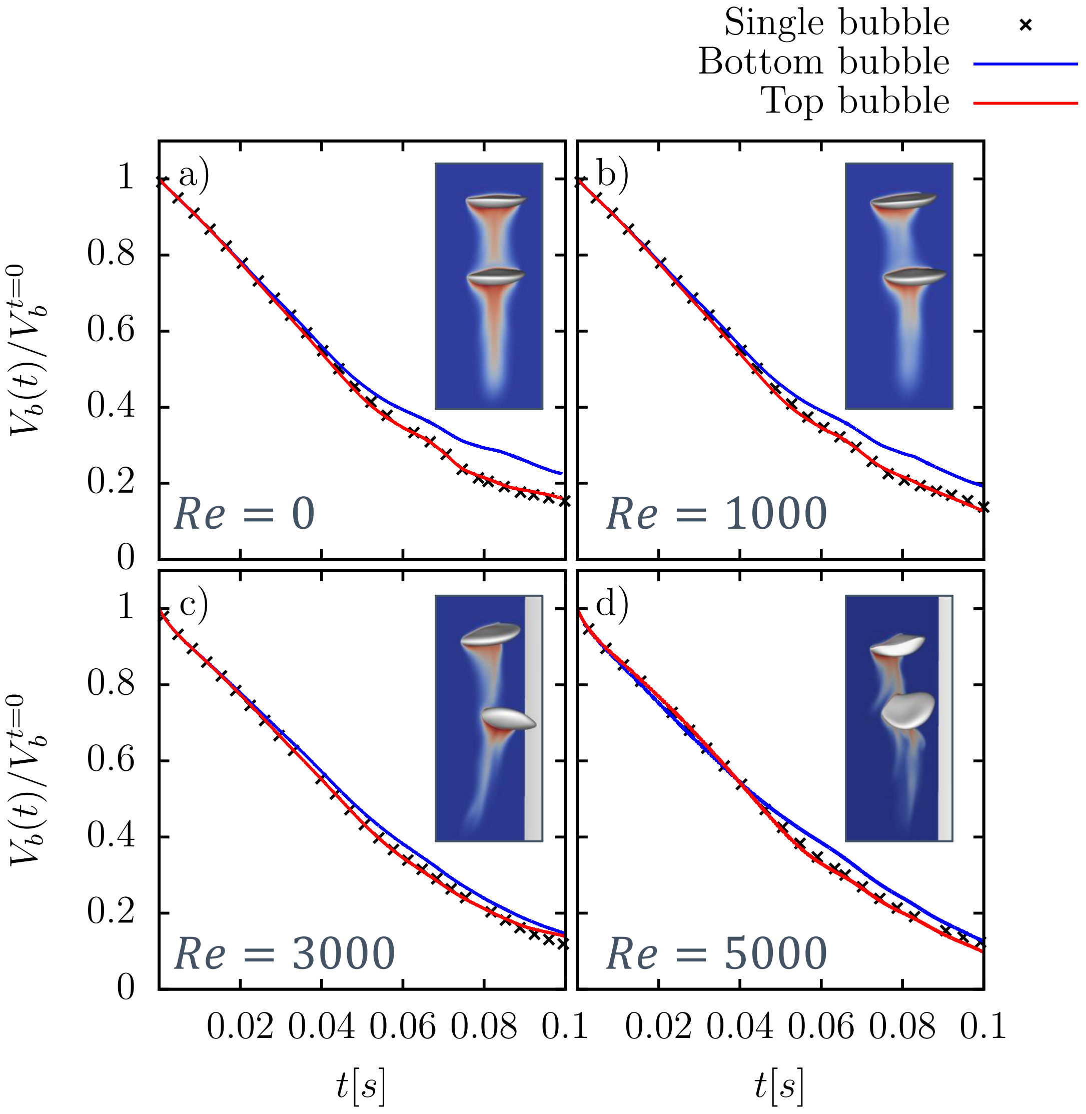

Conclusions

- Numerical framework for the mass transfer of soluble species in two-phase incompressible flows based on Henry's law.
- Redistribution of the mass source term and divergence-free velocity field in interfacial cells.
- Modelling and Validation of laminar and turbulent Taylor-Couette flows
- Large bubbles are less sensitive to the carrier flow (in terms of dissolution rate)
- Standard Sh correlation formulae can provide sensible results when bubbles are mainly driven by gravity
- Stronger Taylor vortices generate more dispersion and enhance global mass transfer for multiple bubbles

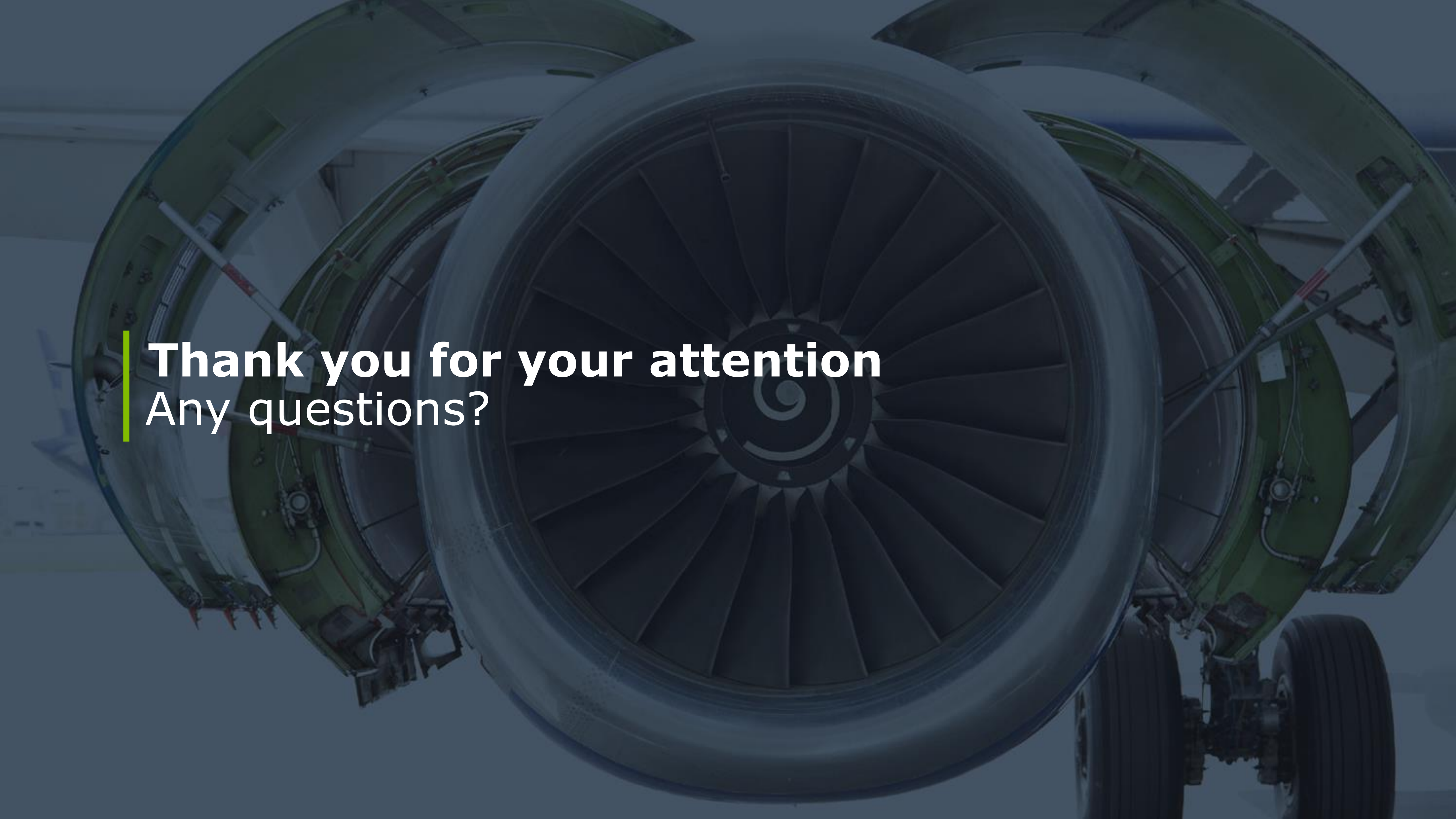

Thank you for your attention

Any questions?